Bulletin of Volcanology (2021) 83: 59
https://doi.org/10.1007/s00445-021-01470-3

RESEARCH ARTICLE

Accumulated Puʻu ʻŌʻō magma fed the voluminous 2018 rift eruption of Kīlauea Volcano: evidence from lava chemistry

Aaron J. Pietruszka[1] · Michael O. Garcia[1] · J. Michael Rhodes[2]

Received: 15 February 2021 / Accepted: 5 June 2021 / Published online: 17 August 2021

Abstract
The 2018 rift eruption of Kīlauea Volcano presents a superb opportunity to decipher the underlying role of magmatic processes on the behavior and hazards of basaltic volcanoes. Here, we examine the petrogenetic history of the most MgO-rich lavas (~ 7.7–8.7 wt.%) from the voluminous (> 0.8 km^3) main phase of this eruption on the volcano's lower East Rift Zone (LERZ). Our results show that these lavas are compositionally homogeneous, but distinct from recent samples of the Puʻu ʻŌʻō eruption on the middle ERZ (MERZ) and the summit lava lake within Halemaʻumaʻu pit crater. The MgO-rich 2018 LERZ lavas have relatively high K_2O and TiO_2 abundances at a given MgO value, high Nb/Y ratios, and low CaO/TiO_2 and Sr/Zr ratios. These observations preclude a simple hypothesis that the collapse of the caldera in 2018 forced magma from the summit reservoir to erupt directly on the LERZ. Instead, the distinctive chemistry of the MgO-rich 2018 LERZ lavas supports a new model of mixing between three components: (1) olivine-controlled magma, derived from the summit reservoir via Puʻu ʻŌʻō, (2) differentiated magma similar to the earliest lavas from the 2018 rift eruption, and (3) olivine. The differentiated magma was stored within the ERZ since the 1960s. The summit-derived magma (~ 91–95%) accumulated downrift of Puʻu ʻŌʻō and mixed with the differentiated magma (~ 5–9%) over ~ 10 years prior to 2018. This process created a large (> 0.8 km^3) magma body within the MERZ that was the direct source of the MgO-rich 2018 LERZ lavas. The magma that was removed from the summit reservoir during the 2018 caldera collapse (up to ~ 0.8 km^3) remains within the ERZ, along with any leftover magma from the Puʻu ʻŌʻō and 2018 rift eruptions. The summit reservoir has likely been replenished with magma based on recent lava lake activity within Halemaʻumaʻu from December 2020 to May 2021. Thus, Kīlauea's plumbing system from the summit to the LERZ may now be flush with magma and primed for a new era of frequent and/or large eruptions.

Keywords Hawaiʻi · Kīlauea · Basalt · Geochemistry · Magma mixing · Rift zone

Introduction

The major hazards of frequently active basaltic volcanoes include rapid and large effusions of lava (e.g., Rhodes 1988; Thordarson and Self, 1993; Clague et al. 1999), violent explosive eruptions (e.g., Fiske et al. 2009; Swanson et al. 2012; Michon et al. 2013; Ort et al. 2016), major earthquakes (e.g., Tilling et al. 1976; Bjarnason et al. 1993; Liu et al. 2018; Chen et al. 2019), and summit or caldera collapse (e.g., Simkin and Howard, 1970; Dvorak 1992; Staudacher et al. 2009). Key aspects of these hazards may be controlled by the enigmatic processes that operate within a volcano's deep magmatic plumbing system (e.g., Pietruszka and Garcia 1999; Sides et al. 2014; Swanson et al. 2014; Pietruszka et al. 2015; Lynn et al. 2017), such as the delivery of new batches of mafic, volatile-rich magma from the mantle, or dynamic changes in the size, location, and interconnectedness of magma bodies. A spectacular and destructive rift eruption occurred at Kīlauea Volcano in mid-2018 (Fig. 1) with the most vigorous, short-duration effusion of lava (> 0.8 km^3 over ~ 3 mo.) in the volcano's ~ 200-year historical record (Neal et al. 2019; Patrick et al. 2020).

Editorial responsibility: N. Métrich

This paper constitutes part of a topical collection: The historic events at Kilauea Volcano in 2018: summit collapse, rift zone eruption, and Mw6.9 earthquake.

✉ Aaron J. Pietruszka
apietrus@hawaii.edu

[1] Department of Earth Sciences, University of Hawaiʻi, Honolulu, HI 96822, USA

[2] Department of Geosciences, University of Massachusetts, Amherst, MA 01003, USA

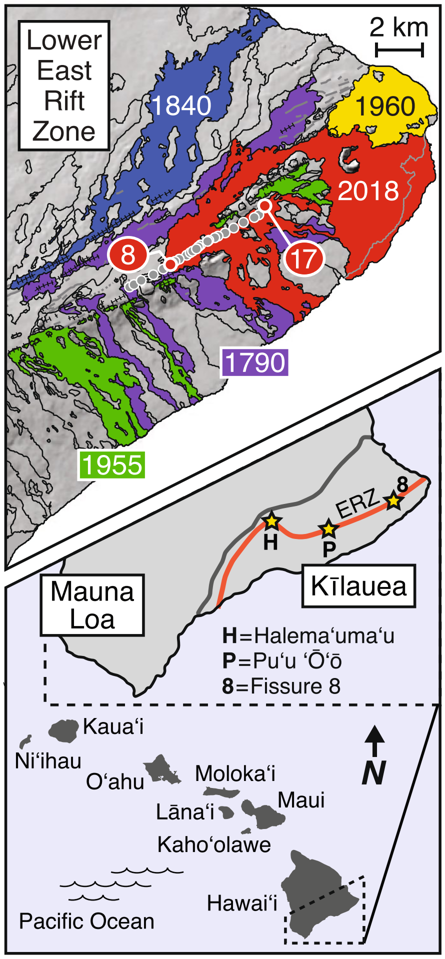

Fig. 1 Map of recent lava flows along the lower East Rift Zone (LERZ) of Kīlauea Volcano (top). Lava flow boundaries, modified from the maps of Trusdell et al. (2005) and Neal et al. (2019), are keyed to the date of eruption and superimposed on a digital elevation map of the volcano. The locations of the 2018 LERZ eruptive fissures from Neal et al. (2019) are shown as gray circles except for fissure 17 and the main fissure 8 (red circles). The locations of Halemaʻumaʻu lava lake ("H"), Puʻu ʻŌʻō vent ("P"), and fissure 8 ("8") are indicated by the yellow stars (bottom)

The 2018 rift eruption coincided with a major (~ 0.8 km^3) summit caldera collapse (Anderson et al. 2019), a M6.9 earthquake beneath the volcano's south flank (Liu et al. 2018; Chen et al. 2019), and the end of two sustained eruptions: (1) the ~ 35-year-long eruption at Puʻu ʻŌʻō on the volcano's East Rift Zone (ERZ) and (2) the ~ 10-year-long summit lava lake within Halemaʻumaʻu pit crater. The 2018 rift eruption produced an unusually large range in lava chemistry (Gansecki et al. 2019), including small amounts of basaltic andesite or andesite (~ 2–4 wt.% MgO) and differentiated basalt (~ 4–7 wt.% MgO), and large amounts of relatively MgO-rich basalt (~ 7–9 wt.%). Thus, Kīlauea's 2018 rift eruption presents a superb opportunity to decipher the underlying role of magmatic processes on the behavior and hazards of basaltic volcanoes.

A preliminary model has emerged from the first studies of the events at Kīlauea in 2018. Immediately prior to the 2018 rift eruption, the volcano's plumbing system (Fig. 2) was pressurized with magma from the summit to the middle ERZ (MERZ), the summit lava lake had recently overflowed onto the floor of Halemaʻumaʻu, and the Hawaiian Volcano Observatory (HVO) had issued multiple warnings that a new vent might open near Puʻu ʻŌʻō (Neal et al. 2019). This situation soon changed dramatically (e.g., Anderson et al. 2019; Neal et al. 2019; Patrick et al. 2019a): (1) the floor of Puʻu ʻŌʻō crater collapsed on April 30 and a dike propagated from the MERZ near Puʻu ʻŌʻō to the lower ERZ (LERZ), (2) the active lava lake within Halemaʻumaʻu began to withdraw on May 1 as the summit deflated, and (3) the new LERZ eruption began on May 3 from fissures located ~ 20 km downrift of Puʻu ʻŌʻō within the Leilani Estates subdivision. The early differentiated lavas that erupted on the LERZ may simply represent leftover magma from a nearby eruption in 1955 that was rapidly flushed out of the rift zone as it mixed with the intruding dike (Gansecki et al. 2019). This hotter, MgO-rich dike magma (represented by the majority of the lava that erupted on the LERZ) was thought to have been supplied directly from Kīlauea's summit reservoir (e.g., Gansecki et al. 2019; Neal et al. 2019; Patrick et al. 2020; Wieser et al. 2021; Lerner et al. 2021), which (prior to 2018) comprised (1) a ~ 2–4-km-deep body beneath the southern rim of the caldera, called the "South Caldera" (SC) magma body, and (2) a < 2-km-deep body beneath the eastern rim of Halemaʻumaʻu (HMM), called the HMM magma body (e.g., Fiske and Kinoshita 1969; Poland et al. 2014; Anderson et al. 2015; Pietruszka et al. 2015; Bemelmans et al. 2021). Collapse of the summit region during the 2018 rift eruption may have forced cooler magma from the shallow HMM body to mix with hotter, deeper magma (up to ~ 13–14 wt.% MgO) within the summit reservoir (e.g., the SC body), or possibly, a deeper portion of the ERZ, prior to transport down the ERZ (Gansecki et al. 2019). A pressure connection between the summit reservoir and the LERZ over ~ 40 km is required by the repeated eruptive surges from the main vent on the LERZ that began within minutes of each episodic caldera collapse event (Patrick et al. 2019a). In detail, however, the nature of the magmatic connection between the summit reservoir and the LERZ in 2018 is poorly understood. Direct links from both the HMM (Neal et al. 2019) and SC (Gansecki et al. 2019; Wieser et al. 2021) magma bodies to the LERZ have been proposed.

Here, we present a new model (Fig. 2) for the magmatic processes that contributed to the 2018 rift eruption using X-ray fluorescence (XRF) measurements of lava and tephra chemistry. The samples used in our study were collected

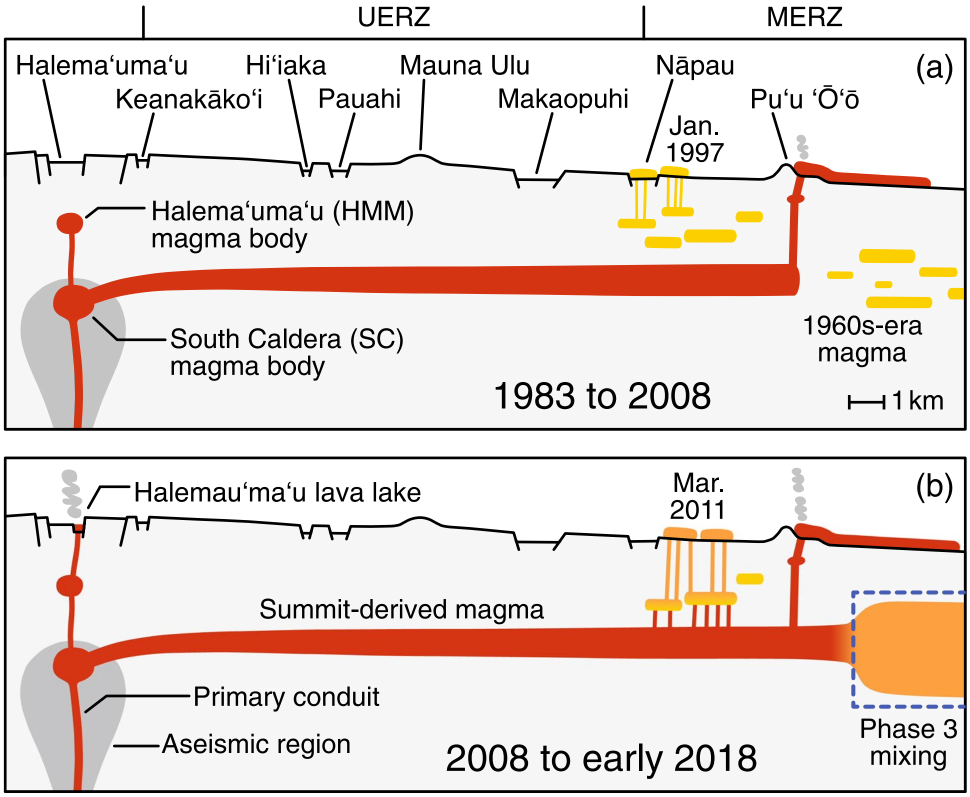

Fig. 2 Schematic cross sections of the magmatic plumbing system of Kīlauea Volcano during the Puʻu ʻŌʻō eruption (Poland et al. 2014; Pietruszka et al. 2018) from (**a**) 1983 to 2008 and (**b**) 2008 to early 2018, just prior to the start of the 2018 rift eruption. A primary conduit delivered mantle-derived magma to the volcano's summit reservoir, which comprised two magma bodies: the shallower Halemaʻumaʻu (HMM) body and the deeper South Caldera (SC) body. The gray area surrounding the SC body marks the volcano's aseismic region (Klein et al. 1987). From 2008 to early 2018, an active lava lake within Halemaʻumaʻu was supplied from the HMM body (itself connected to the SC body), and a dike transported magma from the SC body to Puʻu ʻŌʻō on the East Rift Zone (ERZ). The Puʻu ʻŌʻō vent was underlain by a small (~0.05 km^3) pocket of magma (Shamberger and Garcia 2007). Short-lived eruptions uprift of Puʻu ʻŌʻō in January 1997 and March 2011 tapped a component of differentiated magma that was stored within the ERZ since the 1960s (yellow patches). Our new model in (**b**) posits that a large amount of summit-derived magma accumulated downrift of Puʻu ʻŌʻō over ~ 10 years and mixed with a small amount of stored 1960s-era magma [shown in (**a**)] to create a homogeneous hybrid magma that erupted directly on the LERZ in 2018

from (1) the "last gasp" of the Puʻu ʻŌʻō eruption in May 2018, (2) Halemaʻumaʻu lava lake in 2016 and 2017, and (3) each of the phases of the 2018 rift eruption. These results are compared to the chemistry of lavas from the entire ~ 35-year history of the Puʻu ʻŌʻō eruption (Garcia et al. 1989, 1992, 1996, 2000, 2021; Marske et al. 2008; Greene et al. 2013; Walker et al. 2019) and older historical Kīlauea eruptions (Pietruszka and Garcia 1999; Garcia et al. 2003; Pietruszka et al. 2018). All of these samples were analyzed in the same XRF laboratory. The goals of our study are to (1) establish the petrogenetic history and origin of the MgO-rich lavas from the 2018 rift eruption, (2) infer the evolution of Kīlauea's magmatic plumbing system before and during the 2018 rift eruption, and (3) briefly discuss the implications of our results for the future behavior and hazards of Kīlauea Volcano.

Sampling and analytical methods

The 2018 rift eruption involved 24 fissures on the LERZ (Fig. 1); all but one ("17," the easternmost vent) were aligned in a single ~ 6.8-km-long trend (Neal et al. 2019). The eruption was divided into three phases based on changes in its behavior and lava chemistry [see Gansecki et al. (2019) and Neal et al. (2019) for the details that are summarized here]. Small amounts of differentiated basalt (≤ 7 wt.% MgO) erupted during phase 1 (subdivided as "early," phase 1E, from May 3 to 9, and "late," phase 1L, from May 12 to 18). The most differentiated lava yet known from Kīlauea (except for an accidentally drilled dacite; Teplow et al. 2009), a compositionally heterogeneous basaltic andesite to andesite (~ 55–60 wt.% SiO_2), erupted from fissure 17 (May 13–25, and considered a separate part of phase

1L). We analyzed five samples from phase 1E and four samples from phase 1L (including three from fissure 17). The eruption rate increased during phase 2 (May 17 to 27) and the lava rapidly became richer in MgO (up to ~ 8 wt.%). During phase 3 (May 28 to August 4), the eruption focused at fissure 8 with the rapid (50–200 m^3/s) and voluminous (> 0.8 km^3) effusion of relatively homogeneous, MgO-rich lava (~ 7–9 wt.%). We analyzed four samples from phase 2 (two from fissure 8) and 17 samples that span the entirety of phase 3 (all from fissure 8). Additionally, the "last gasp" sample of lava from Puʻu ʻŌʻō (erupted on May 1, 2018) and two samples from Halemaʻumaʻu lava lake (one overflow onto the floor of the crater in January 2016 and one sample of tephra from April 2017) were analyzed. The 2017 tephra was limited in volume, and thus, not analyzed for trace element abundances.

All of the samples (n = 33) were collected near the active vents by HVO scientists and volunteers, and rapidly quenched to inhibit post-eruptive crystallization either in the air for spatter (S) samples or with water for most of the flow (F) samples. Mineral modes for a subset of the samples (n = 10) from the 2018 rift eruption were determined by point counting (n = 500 each, excluding vesicles) under a petrographic microscope (Supplementary Table S1). The major and trace element abundances of the samples and reference materials (Supplementary Table S2) were measured by XRF at the University of Massachusetts (UM) using the methods of Rhodes and Vollinger (2004). A new XRF instrument (a Panalytical Zetium Ultimate) was calibrated and used to determine the major element abundances of the samples. A comparison of reference materials (BHVO-2 and K1919) analyzed on the new XRF instrument during this study with previous measurements (Pietruszka et al. 2013, 2018) indicates that the major element abundances agree within ~ 0.5–1% relative for SiO_2, Al_2O_3, and CaO; ~ 2% for Fe_2O_3, MgO, TiO_2, and K_2O; ~ 4% for P_2O_5; and ~ 11–12% for MnO and Na_2O. The eruption date and location of each sample is provided in Supplementary Table S2. To avoid potential complications from interlaboratory bias and the use of both wavelength- and energy-dispersive XRF instruments by Gansecki et al. (2019), we show only data collected using wavelength-dispersive XRF at UM on the figures. However, the observations and interpretations of Gansecki et al. (2019) for the 2018 rift eruption are described in the following discussion of our new results.

Results

Lavas from the 2018 rift eruption range widely in composition (Fig. 3a) from the basaltic andesite to andesite (~ 2.3–3.4 wt.% MgO in this study) at fissure 17 to the relatively MgO-rich basalt that dominated phase 3 at fissure 8 (~ 7.7 to 8.7 wt.%). The phase 1 early (~ 4.6–4.9 wt.% MgO) and late (~ 5.8 wt.% for one sample, excluding those from fissure 17) lavas are differentiated (defined as ≤ 7 wt.% MgO due to fractionation beyond olivine control; Wright 1971; Wright and Fiske 1971). The phase 1E samples are virtually aphyric with only sparse (< 2 vol.%) microphenocrysts (0.1–0.5 mm) of plagioclase and clinopyroxene, whereas the phase 1L sample also has rare (< 1 vol.%) phenocrysts (> 0.5 mm) of these minerals. Plagioclase crystals with sieve textures are present in the phase 1 samples (Fig. 4a), indicating crystal-melt disequilibrium. Ilmenite was observed in the phase 1E lavas by Gansecki et al. (2019). The MgO contents of the phase 2 lavas (~ 7.0–8.1 wt.%) are lower (on average) than the phase 3 lavas (Fig. 3a). The phase 2 and 3 lavas from fissure 8 are richer in MgO (~ 7.5 to 8.7 wt.%) than the final sample of the Puʻu ʻŌʻō eruption from May 2018 (~ 6.9 wt.%) and the two samples from Halemaʻumaʻu lava lake in 2016 and 2017 (~ 7.4 and 7.0 wt.%, respectively). The phase 2 and early phase 3 samples (until mid-June) have (1) phenocrysts and microphenocrysts of olivine, clinopyroxene, and plagioclase (variable amounts, but up to ~ 1–4 vol.% of each mineral), (2) rare (~ 1 vol.%) open-textured gabbro crystal clots (Fig. 4b–c), and/or (3) sieve-textured plagioclase crystals (Fig. 4d). Olivine is the dominant phenocryst and microphenocryst for most of the subsequent phase 3 samples (Fig. 4e–f). These later samples lack gabbro crystal clots or signs of plagioclase disequilibrium. The modal abundances of olivine in the phase 3 samples do not correlate with their MgO contents.

The differentiated lavas from phase 1 of the 2018 rift eruption have more variable and much higher abundances of incompatible elements (e.g., K_2O), lower CaO/TiO_2 ratios, and higher Nb/Y ratios than the lavas from phases 2 and 3 or recent lavas from Puʻu ʻŌʻō and Halemaʻumaʻu (Fig. 3b–d). In contrast, the phase 2 and 3 lavas are relatively homogeneous in composition and broadly similar to recent lavas from Puʻu ʻŌʻō and Halemaʻumaʻu. However, the MgO-normalized (i.e., fractionation-corrected to 10 wt.% MgO) K_2O (Fig. 3e) and TiO_2 (not shown) abundances of the phase 2 and 3 lavas from fissure 8 are significantly higher than recent lavas from Puʻu ʻŌʻō and Halemaʻumaʻu, a difference that was previously noted by Gansecki et al. (2019). These differences in lava chemistry extend to CaO/TiO_2 (which shows a small, but systematic, fluctuation) and Nb/Y (Fig. 3f–g).

Discussion

The first studies of the 2018 rift eruption suggested that the phase 2 and 3 lavas from fissure 8 (hereafter called the "MgO-rich 2018 LERZ lavas") were supplied directly from

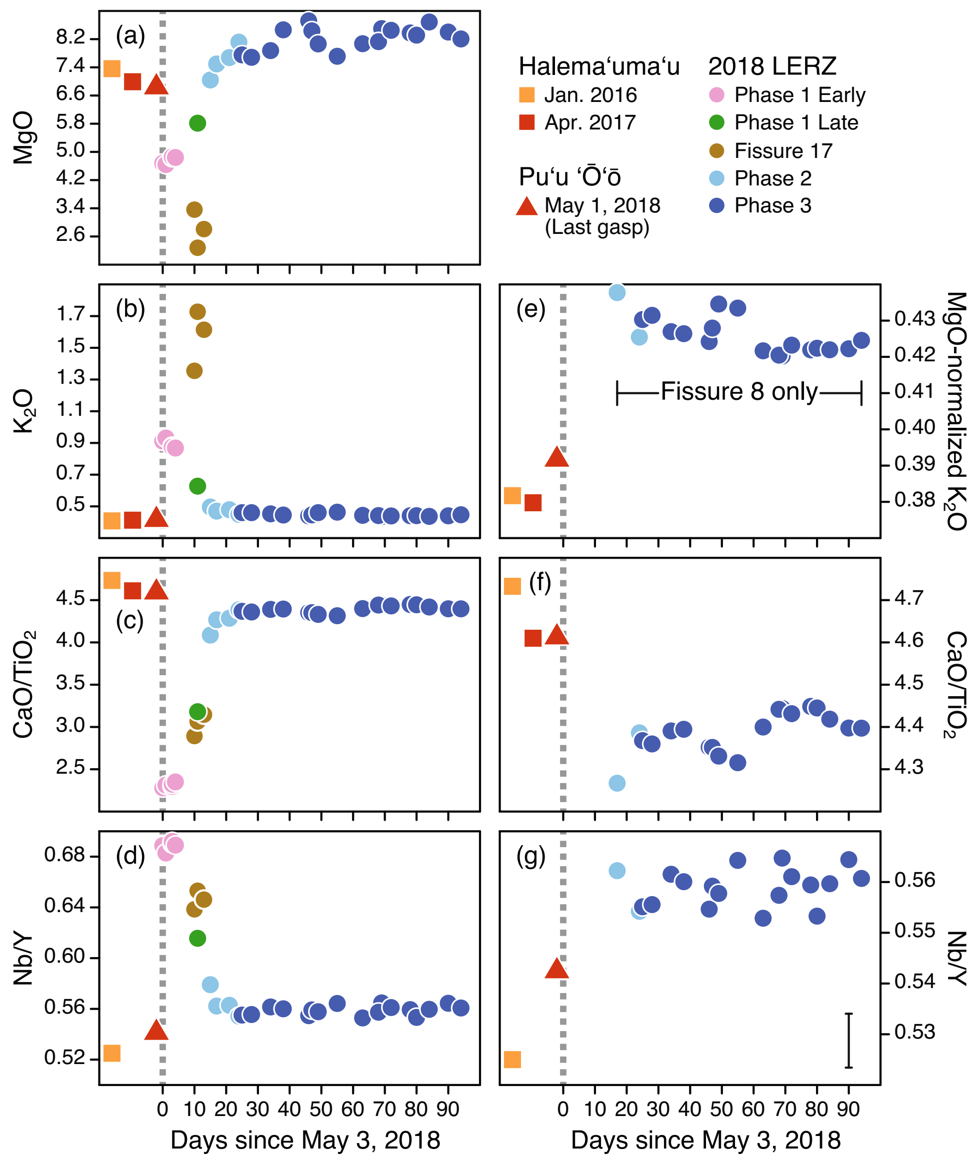

Fig. 3 Temporal variations in lava chemistry at Kīlauea prior to (2016 to 2018) and during the 2018 rift eruption. Samples from the entire 2018 rift eruption are shown in the plots on the left (**a–d**), whereas the plots on the right (**e–g**) include only the phase 2 and 3 samples from fissure 8 in addition to the recent samples from Halema'uma'u and Pu'u 'Ō'ō. All data are from Supplementary Table S2. The MgO-normalized K_2O abundances of the samples with ≥ 7.0 wt.% MgO (except for the "last gasp" Pu'u 'Ō'ō sample with 6.9 wt.% MgO) were calculated by adding small amounts of equilibrium olivine in steps of 0.5 mol.% until the MgO content of the mixture reached 10 wt.% [using the Fe–Mg partitioning Kd = 0.30 from Roeder and Emslie (1970)]. Similar trends would be obtained using a slightly higher Kd value of ~ 0.34 based on experiments for Hawaiian tholeiitic basalts (Matzen et al. 2011). Element abundances are in wt.%. Ratios of major or trace elements are in proportions of wt.% or ppm, respectively. The 2SD error bar for Nb/Y is shown in (**g**); the other error bars are smaller than the size of the symbols

Kīlauea's summit reservoir to the LERZ (e.g., Gansecki et al. 2019; Neal et al. 2019; Patrick et al. 2020; Wieser et al. 2021; Lerner et al. 2021). In this discussion, we critically evaluate this preliminary model in four steps using lava chemistry. First, the distinctive chemistry of the MgO-rich 2018 LERZ lavas is described, and their petrogenetic history is deciphered. Second, an alternative two-stage model that involves (1) magma mixing within the ERZ over ~ 10 years prior to the 2018 rift eruption followed by (2) olivine accumulation shortly before or during the eruption is proposed. Third, the potential end-member magmas that mixed to create the homogeneous hybrid magma that erupted on the LERZ in 2018 are identified. Fourth, the location (downrift of Pu'u 'Ō'ō) and size (> 0.8 km^3) of the ERZ magma body that directly supplied the 2018 rift eruption is inferred (Fig. 2). Finally, the broader implications of our results for the future behavior and hazards of Kīlauea Volcano are briefly explored.

The distinctive chemistry of the MgO-rich 2018 LERZ lavas

The distinctive chemistry of the MgO-rich 2018 LERZ lavas is well illustrated by comparison with the temporal evolution of lavas from the Pu'u 'Ō'ō eruption since 1985 (i.e., after the end of the early period of magma mixing within the ERZ; Garcia et al. 1989, 1992). Specifically, the MgO-rich 2018 LERZ lavas have (1) higher MgO contents (~ 7.5–8.7 wt.%; Fig. 5a) than most Pu'u 'Ō'ō lavas from the last decade (e.g., ~ 6.5 to 7.8 wt.% since March 2011) and (2) lower CaO/TiO_2 ratios (Fig. 5b) than nearly all samples from the main episodes of the Pu'u 'Ō'ō eruption (excluding the early

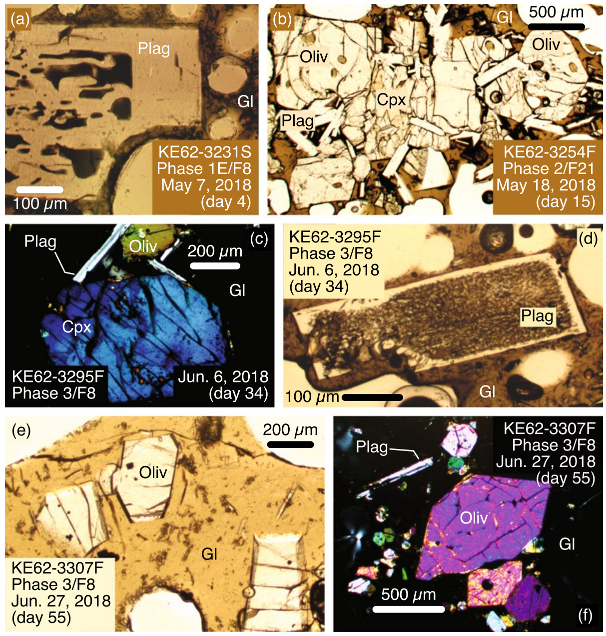

Fig. 4 Photomicrographs of lava samples from the 2018 rift eruption of Kīlauea Volcano. Examples from phase 1E (**a**), phase 2 (**b**), and phase 3 (**c–f**) of the eruption are discussed in the text. Images (**c**) and (**f**) were taken in cross-polarized light. Abbreviations: olivine (Oliv); plagioclase (Plag); clinopyroxene (Cpx); glass (Gl); fissure number (F)

mixing-dominated lavas that erupted prior to February 1985, and the two brief uprift eruptions of stored, differentiated magma in January 1997 and March 2011 that are not shown on Fig. 5). The MgO-rich 2018 LERZ lavas also have MgO-normalized TiO_2 abundances (Fig. 5c) that are (1) higher than recent Puʻu ʻŌʻō lavas but (2) similar to Puʻu ʻŌʻō samples from the mid-1980s to mid-1990s. The relatively high Nb/Y ratios (~0.56 on average) of the MgO-rich 2018 LERZ lavas (Fig. 3g) seem to continue (and extend) the recent temporal increase in Nb/Y from a minimum of ~0.49 in the early 2000s to ~0.54 in 2018 (Fig. 5d). A higher Nb/Y ratio of ~0.56 was last observed in Puʻu ʻŌʻō samples from the late 1980s to early 1990s. The MgO-rich 2018 LERZ lavas are similarly distinct from the 2016 and 2017 Halemaʻumaʻu samples, which are similar to contemporaneous Puʻu ʻŌʻō lavas (Fig. 5).

Recent Puʻu ʻŌʻō lavas from 2011 to 2018 (including the "last gasp" sample from May 2018) and Halemaʻumaʻu samples from 2016 and 2017 likely represent the chemistry of magma within Kīlauea's summit reservoir prior to the 2018 rift eruption. These lavas plot along trends of magmatic differentiation from a common parental magma (Fig. 6) that was calculated from recent olivine-controlled Puʻu ʻŌʻō samples as described in the caption to Fig. 6. A subset of Puʻu ʻŌʻō samples with unusually low TiO_2 abundances (Fig. 6a), high Al_2O_3 (Fig. 6b) and CaO (Fig. 6c) abundances, and high CaO/TiO_2 ratios (Fig. 6d) that accumulated small open-textured gabbro crystal clots (shown by dashed red fields on Fig. 6) do not plot along the differentiation trends. These anomalous samples are not discussed further or shown on other figures [see Garcia et al. (2021) for more information]. The MgO-rich 2018 LERZ lavas plot within the differentiation trends only for Al_2O_3. Notably, the TiO_2 abundances of these lavas at a given MgO value are significantly higher than recent lavas from Puʻu ʻŌʻō and Halemaʻumaʻu and, instead, overlap with samples from the earliest part of the Puʻu ʻŌʻō eruption (mid-1980s to mid-1990s). This is consistent with their relatively high MgO-normalized TiO_2 abundances (Fig. 5c). These observations indicate that the MgO-rich 2018 LERZ lavas cannot be derived from the same parental magma as recent lavas from Puʻu ʻŌʻō and Halemaʻumaʻu by variable amounts of differentiation. Thus, their distinctive chemistry precludes the simple hypothesis that the collapse of the caldera in 2018 forced magma from the summit reservoir to erupt directly on the LERZ (e.g., Gansecki et al. 2019; Neal et al. 2019; Patrick et al. 2020; Wieser et al. 2021; Lerner et al. 2021).

An alternative hypothesis posits that the caldera collapse forced cooler magma from the shallow portion of the summit reservoir (beneath Halemaʻumaʻu) to mix with hotter, deeper magma in the summit reservoir or, possibly, a deeper portion of the ERZ, prior to transport of the mixed magma down the ERZ (Gansecki et al. 2019). The chemistry of these deeper magmas is unknown. In this scenario, however, the higher abundances of incompatible elements in the MgO-rich 2018 LERZ lavas (e.g., TiO_2) might record the involvement of a new, compositionally distinct batch of olivine-controlled magma from the mantle. This idea of mixing with a hot, deep magma batch might also explain (1) the relatively high Nb/Y ratios of the MgO-rich 2018 LERZ lavas (Fig. 3g), which seem to continue (and extend) the temporal trend of increasing Nb/Y that is defined by recent Puʻu ʻŌʻō samples (Fig. 5d), and (2) the heterogeneous olivine population in the MgO-rich 2018 LERZ lavas, including crystals with Fo_{88-89} cores that must have formed in equilibrium with a relatively primitive (~13–14 wt.% MgO) melt (Gansecki et al. 2019). However, the low CaO/TiO_2 ratios of the MgO-rich 2018 LERZ lavas compared to nearly all olivine-controlled Puʻu ʻŌʻō samples (Fig. 5b) are inconsistent with the idea of mixing between two magmas that never differentiated beyond olivine control. Furthermore, the CaO abundances (Fig. 6c) and CaO/TiO_2 ratios (Fig. 6d) of the MgO-rich 2018 LERZ lavas are lower at a given MgO value than the predicted trends of magmatic differentiation for recent Puʻu ʻŌʻō or Halemaʻumaʻu lavas. These observations suggest that the MgO-rich 2018 LERZ lavas include at least one component of magma that fractionated clinopyroxene ± plagioclase. This differentiated magma would be expected to have a relatively low CaO abundance and CaO/TiO_2 ratio and relatively high abundances of incompatible elements.

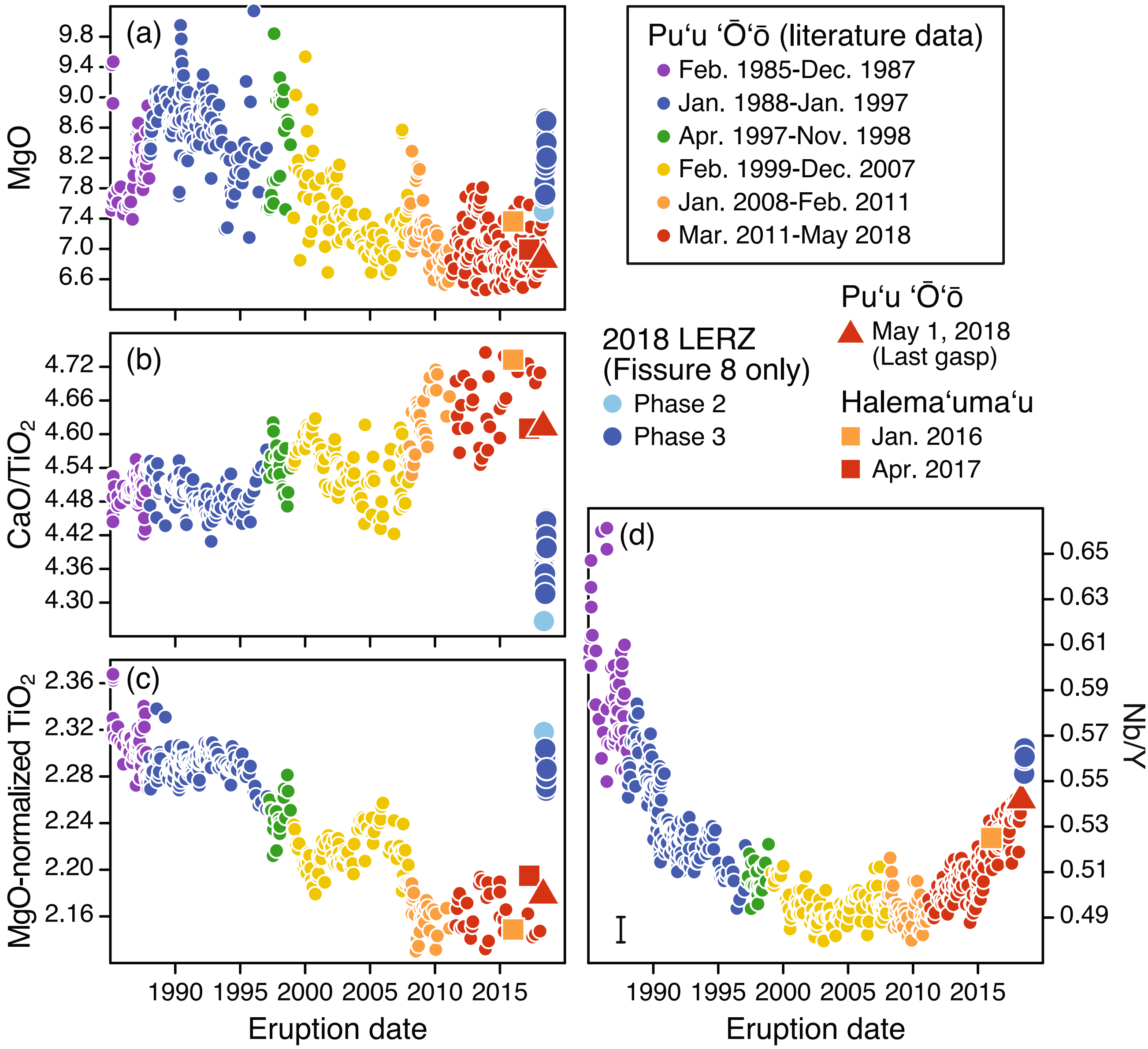

Fig. 5 Temporal variations in lava chemistry at Kīlauea since 1985. Samples from fissure 8 of the 2018 rift eruption (phases 2 and 3) and recent samples from Halema‘uma‘u (2016 and 2017) and Pu‘u ‘Ō‘ō (2018) are compared to the main episodes of the Pu‘u ‘Ō‘ō eruption from 1985 to 2018. Data from Supplementary Table S2 (large symbols) are compared with literature data (small symbols) for the Pu‘u ‘Ō‘ō eruption (Garcia et al. 1992, 1996, 2000, 2021; Marske et al. 2008; Greene et al. 2013). Pu‘u ‘Ō‘ō samples from the early mixing-dominated episodes prior to February 1985 and the two uprift eruptions of differentiated magma in January 1997 and March 2011 are not shown. Thus, these plots emphasize the temporal variations in the MgO abundances of Pu‘u ‘Ō‘ō lavas (**a**), and the composition of the parental magma delivered to Pu‘u ‘Ō‘ō from the summit reservoir (**b–d**) for comparison with the recent samples from Pu‘u ‘Ō‘ō, Halema‘uma‘u, and the LERZ (fissure 8). The MgO-normalized TiO_2 abundances of the samples (**c**) were calculated as described in the caption to Fig. 3. Samples with < 7.0 wt.% MgO are also excluded from (**b**) to avoid the effect of differentiation beyond olivine control on the CaO/TiO_2 ratios of the lavas. Additionally, a subset of recent Pu‘u ‘Ō‘ō samples with unusually low TiO_2 abundances, high Al_2O_3 and CaO abundances, and high CaO/TiO_2 ratios that accumulated small open-textured gabbro crystal clots are not shown (see the caption to Fig. 6 for more details). Element abundances are in wt.%. Ratios of major or trace elements are in proportions of wt.% or ppm, respectively. The 2SD error bar for Nb/Y is shown; the other error bars are smaller than the size of the symbols

Thus, the distinctive chemistry of the MgO-rich 2018 LERZ lavas—with their high MgO (Fig. 3a), TiO_2 (Fig. 5c), and K_2O (Fig. 3e) abundances, and low CaO/TiO_2 ratios (Fig. 5b) compared to recent Pu‘u ‘Ō‘ō or Halema‘uma‘u samples—is probably unrelated to the involvement of a new, hotter, deeper summit-derived magma.

Instead, we explore the hypothesis that these chemical signatures are related to magma mixing within

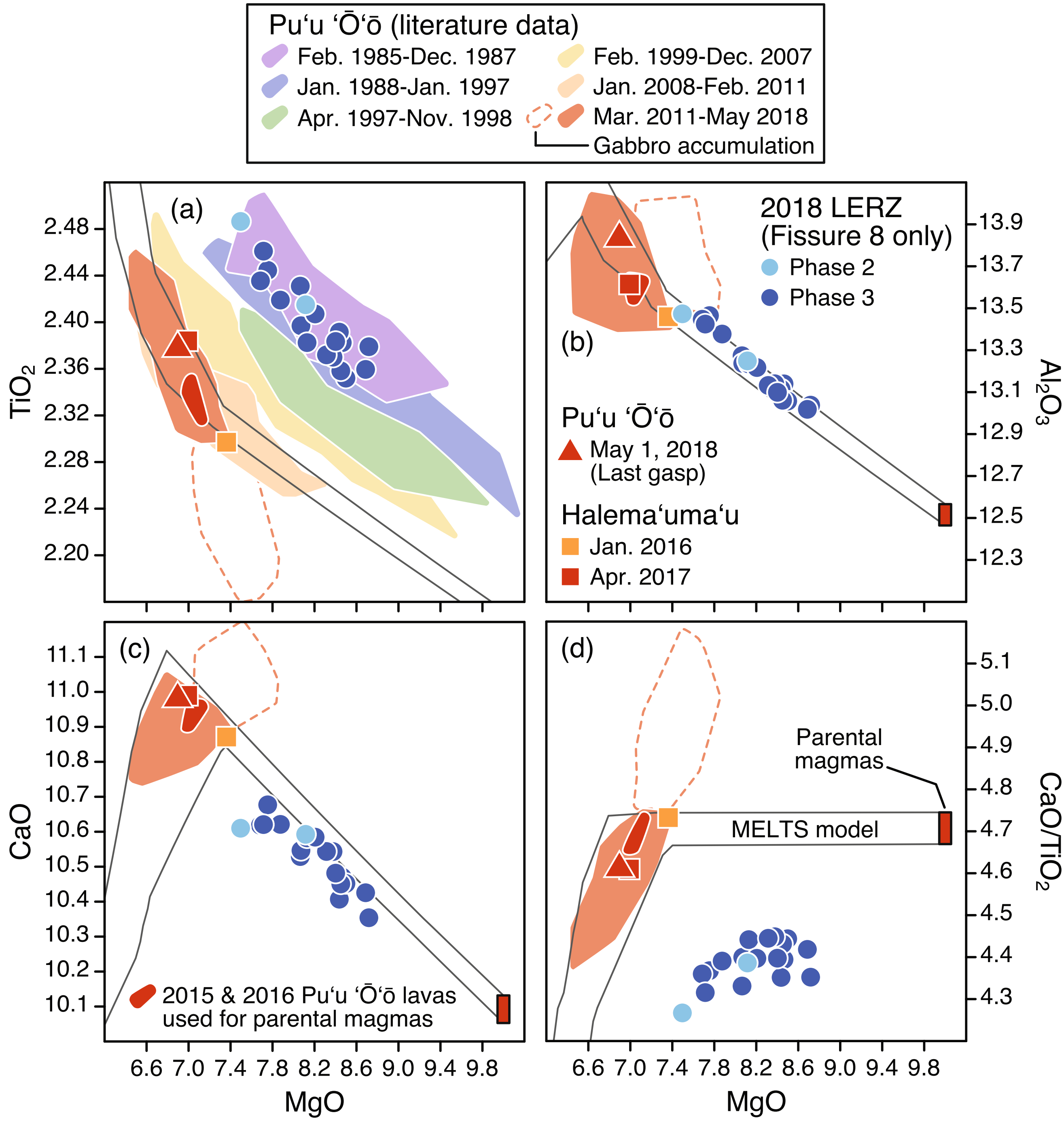

the ERZ prior to the 2018 rift eruption. This mixing process (Fig. 2) involved a large amount of summit-derived magma that accumulated downrift of Pu‘u ‘Ō‘ō over ~ 10 years and a small amount of differentiated, rift-stored magma from the 1960s. Two other potential models for the distinctive chemistry of the MgO-rich 2018 LERZ lavas—related to (1) rapid, syn-eruptive cooling and differentiation of contemporaneous summit-derived magma during its transport down the ERZ in 2018 (to create a low CaO/TiO_2 ratio) or (2) the eruption of an older, high-TiO_2 Pu‘u ‘Ō‘ō magma (purple and blue fields on Fig. 6a) that was stored and differentiated within the ERZ for ~ 20–30 years—are considered and rejected in the Supplementary Information.

Evidence for two stages of mixing

The distinctive chemistry of the MgO-rich 2018 LERZ lavas can be explained by mixing between three components (Fig. 7): (1) recent magma derived from the summit

◂**Fig. 6** MgO variation diagrams for samples of lava from fissure 8 of the 2018 rift eruption of Kīlauea Volcano (phases 2 and 3), and recent samples from Halemaʻumaʻu (2016 and 2017) and Puʻu ʻŌʻō (2018) with trends of magmatic differentiation from recent Puʻu ʻŌʻō parental magmas. Data from Supplementary Table S2 (symbols) are compared with literature data for the main episodes of the Puʻu ʻŌʻō eruption (fields) from 1985 to 2018 (see the caption to Fig. 5 for data sources). A subset of recent lava samples from Puʻu ʻŌʻō since 2011 have unusually low TiO_2 abundances (**a**), high Al_2O_3 (**b**) and CaO (**c**) abundances, and high CaO/TiO_2 ratios (**d**). These signatures are thought to be related to the accumulation of small open-textured gabbro crystal clots at shallow levels of the magmatic plumbing system and/or during the eruption and flow of the lava. Accordingly, Puʻu ʻŌʻō samples with $CaO/TiO_2 > 4.75$ are enclosed by the dashed red fields and excluded from subsequent figures and discussion. Fields for Puʻu ʻŌʻō samples prior to March 2011 are omitted from (**b**–**d**). The compositional range of recent Kīlauea parental magmas (red boxes) was estimated by adding small amounts of equilibrium olivine to olivine-controlled Puʻu ʻŌʻō lava samples (red fields) from 2015 (April 23, 2015, and June 16, 2015) and 2016 (April 14, 2016) until the MgO content of the mixture reached 10 wt.% (see the caption to Fig. 3 for the method). These 2015 and 2016 parental magmas were used as starting compositions for MELTS modeling (Ghiorso and Sack 1995; Gualda et al. 2012) to produce a range of differentiated magmas shown in the white trends. For each parental magma, the MELTS model parameters were 0.2 wt.% H_2O, and four combinations of two redox conditions (QFM or QFM-1) and two pressures (0.5 and 1.0 kbar). The crystals that formed during each increment of cooling (1 °C) were assumed to fractionate from the residual melt. The parental magma in (**a**) lies off the scale of the plot. All values are in wt.%. The 2SD error bars are smaller than the size of the symbols

reservoir, (2) differentiated, rift-stored magma similar to the phase 1E lavas from 2018 (i.e., the differentiated magma component), and (3) olivine. Magma similar to the basaltic andesites and andesites that erupted from fissure 17 can be excluded as a mixing component because their TiO_2 abundances are far too low due to the fractionation of Fe-Ti oxides (brown arrow on Fig. 7a). The phase 1L lava probably represents an intermediate hybrid magma (Gansecki et al. 2019) and is not considered further. In contrast, the phase 1E lavas represent a potential mixing end member. They have Al_2O_3 abundances (Fig. 7b) that are similar to recent summit or Puʻu ʻŌʻō samples (at a lower MgO content), but much higher TiO_2 (Fig. 7a) and lower CaO (Fig. 7c) abundances, and much lower CaO/TiO_2 ratios (Fig. 7d).

The major element variations of the MgO-rich 2018 LERZ lavas require two stages of mixing: (1) initial two-component magma mixing to create a relatively homogeneous hybrid magma followed by (2) the addition of variable amounts of olivine. This process is illustrated (Fig. 7) using the "last gasp" Puʻu ʻŌʻō sample from May 2018 to represent magma derived from the summit reservoir, but many other recent Puʻu ʻŌʻō lavas (red fields) and the April 2017 sample from Halemaʻumaʻu lava lake are suitable choices. First, the summit-derived magma is mixed with the average composition of the phase 1E lavas to create a hybrid magma (green bars along the mixing trends on Fig. 7). The range in mixing proportions is calculated to match the CaO/TiO_2 ratios of the MgO-rich 2018 LERZ lavas from phase 3 (~4.32–4.45), since this parameter is virtually invariant during the fractionation or accumulation of olivine. A total of ~91–95 wt.% summit-derived magma and ~5–9 wt.% differentiated phase 1E magma is required if either the May 2018 Puʻu ʻŌʻō sample or April 2017 Halemaʻumaʻu sample is used for the calculation because they have similar CaO/TiO_2 ratios. This mixing process will create a hybrid magma with a higher TiO_2 abundance (Fig. 7a), and lower CaO abundance (Fig. 7c) and CaO/TiO_2 ratio (Fig. 7d) than the summit-derived magma, with little change in Al_2O_3 (Fig. 7b). Second, a variable amount of olivine is added to increase the MgO content of the hybrid magma and match the range in the chemistry of the MgO-rich 2018 LERZ lavas from phase 3 (green fields for Fo82 to Fo88 on Fig. 7). A total of ~2–6 wt.% olivine accumulation is required. Samples of lava from fissure 8 during phase 3 of the 2018 rift eruption (June to August) contain up to ~3 vol.% olivine phenocrysts and ~6 vol.% olivine microphenocrysts on a vesicle-free basis (Supplementary Table S1). This two-stage mixing model is attractive because it explains the distinctive chemistry of the MgO-rich 2018 LERZ lavas by mixing three components (two lavas and a heterogeneous olivine population) that were observed to erupt at Kīlauea. In this scenario, the high-Fo olivine crystals in the MgO-rich 2018 LERZ lavas (Gansecki et al. 2019; Wieser et al. 2021) likely accumulated shortly before or during the eruption, which is a common magmatic process within Kīlauea's summit reservoir (Garcia et al. 2003; Wieser et al. 2019) and ERZ (e.g., Clague et al. 1995; Vinet and Higgins 2010; Tuohy et al. 2016). The viability of this model is further demonstrated by the low residuals for the two-stage mixing calculation on a sample-by-sample basis (Supplementary Table S3).

There are two lines of evidence to support the idea that the first stage of magma mixing occurred prior to the 2018 rift eruption. First, the MgO-rich 2018 LERZ lavas from phase 3 are relatively homogeneous (Fig. 3) with a total variation of only ~2–3% (relative) in MgO-normalized K_2O (**Fig. 3e**) and TiO_2 (Fig. 5c), CaO/TiO_2 (Fig. 3f), and Nb/Y (Fig. 3g). The limited variation in the chemical parameters that are insensitive to olivine accumulation or fractionation—despite the large differences in the composition of the (inferred) magma mixing end members (Fig. 7)—indicates that the MgO-rich 2018 LERZ lavas were well mixed prior to eruption. The alternative hypothesis—syn-eruptive homogenization of > 0.8 km^3 of magma within the ERZ—would require a delicate (and unlikely) balance in the mixing proportions of the summit-derived (~91–95 wt.%) and rift-stored (~5–9 wt.%) magmas on the time scale of the 2018 rift eruption itself (i.e., ~2 months for phase 3). This is especially difficult given the narrow (~2–3 m) width of the conduit that fed

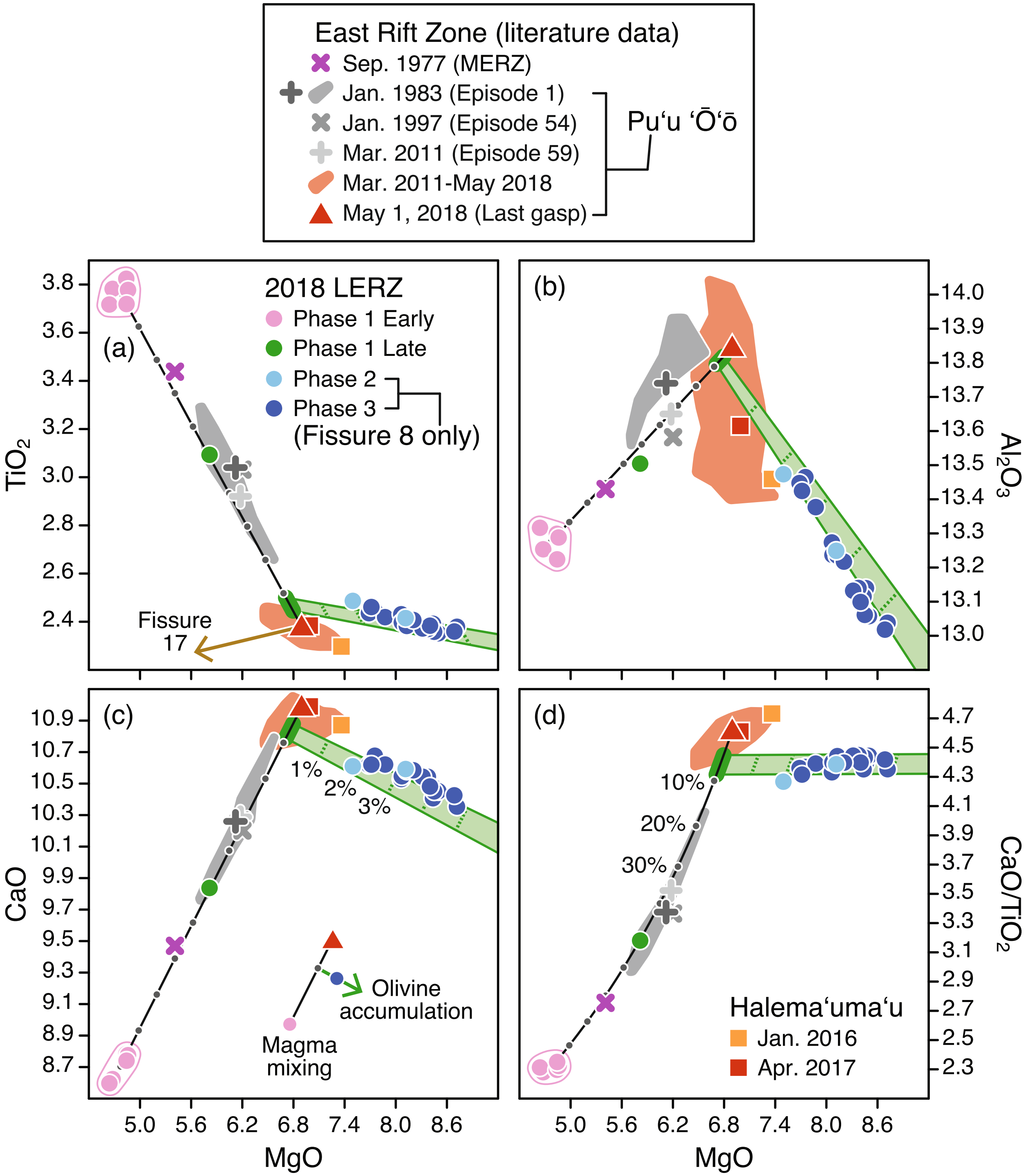

Pu‘u ‘Ō‘ō from the summit reservoir (Patrick et al. 2019b). Second, the dominant compositional variations of MgO-rich 2018 LERZ lavas (e.g., ~ 13% relative range in MgO due to the accumulation of olivine) are orthogonal to the trend expected for mixing between recent summit-derived magma and the phase 1E magma (Fig. 7). The importance of this point is further illustrated by contrast with the mixing trends for episode 1 lavas from the Pu‘u ‘Ō‘ō eruption in January 1983 (gray fields on Fig. 7), which were interpreted to result from a “hydraulic plunger” as summit-derived magma intruded the ERZ and forced two differentiated, rift-stored magmas to mix and erupt (Garcia

◂**Fig. 7** Two-stage mixing model for the lavas from phase 3 of the 2018 rift eruption of Kīlauea Volcano. The plots show MgO vs. **a** TiO_2, **b** Al_2O_3, **c** CaO, and **d** CaO/TiO_2 for samples from phase 1 (early and late) and fissure 8 (phases 2 and 3) of the 2018 rift eruption and recent samples from Halema'uma'u (2016 and 2017) and Pu'u 'Ō'ō (2018). These data from Supplementary Table S2 (symbols, except the crosses) are compared with (1) literature data for four samples (crosses) from the MERZ (September 1977, sample 1–54 from episode 1 of the Pu'u 'Ō'ō eruption in 1983, the average of samples from episode 54 of the Pu'u 'Ō'ō eruption in 1997, and the average of the more differentiated group of samples from episode 59 of the Pu'u 'Ō'ō eruption in 2011) and (2) Pu'u 'Ō'ō lavas (fields) from episode 1 and March 2011 to May 2018. The literature data sources are listed in the caption to Fig. 5, except for the samples from episodes 54 and 59 (Walker et al. 2019). The first stage of magma mixing is shown between the May 2018 "last gasp" Pu'u 'Ō'ō lava and the average of the phase 1E samples from the 2018 rift eruption. The range in the proportions of these two magmas is calculated to match the minimum (~4.32) and maximum (~4.45) CaO/TiO_2 ratios of the lavas from phase 3 of the 2018 rift eruption (dark blue circles). The small gray circles show 10 wt.% increments of magma mixing. The second stage of olivine accumulation (green fields) was calculated by adding Fo82 or Fo88 (in bulk) to these hybrid magmas. This range is based on Gansecki et al. (2019): (1) Fo82 is the average of all measured olivine cores from phase 3 of the 2018 rift eruption and (2) Fo88 is the average subset of these olivine cores with ≥ Fo87. The dashed green lines show 1 wt.% increments of Fo88 addition. Element abundances are in wt.%. Ratios of major elements are in proportions of wt.%. The 2SD error bars are smaller than the size of the symbols

et al. 1989). Evidence for syn-eruptive magma mixing in 2018 is observed in the phase 1 and early phase 2 lavas (Gansecki et al. 2019), excluding those from fissure 17 (Fig. 7a), based on (1) the temporal trends in lava chemistry during the first ~ 20 days of the eruption (e.g., left panels on Fig. 3) and (2) the intermediate position of the phase 1L sample on the mixing trends (Fig. 7). However, the amount of lava affected by this syn-eruptive mixing likely represents a small fraction of the total lava output in 2018, which mostly (~ 92–96%) erupted during phase 3 (Gansecki et al. 2019).

Mixing with differentiated 1960s-era magma in the ERZ

The temporal evolution in Nb/Y for historical Kīlauea summit and rift lavas (Fig. 8a) can be used to identify the differentiated magma component and confirm an ERZ location for the first stage of mixing. The Nb/Y ratios of Kīlauea lavas increased from the early to mid-twentieth century (gray to green squares on Fig. 8b, respectively) and reached a maximum value after the collapse of Halema'uma'u lava lake in 1924 (Pietruszka and Garcia 1999; Garcia et al. 2003), and then decreased to a minimum value during the Pu'u 'Ō'ō eruption, early in the first decade of the twenty-first century (Greene et al. 2013). Subsequently, the Nb/Y ratios of Pu'u 'Ō'ō (Garcia et al. 2021) and Halema'uma'u lavas increased slightly (Fig. 5d). The phase 1E lavas from the 2018 rift eruption have much higher Nb/Y ratios than (1) recent samples from Halema'uma'u (since 2016), (2) the main episodes of Pu'u 'Ō'ō eruption (since 1988), and (3) summit and ERZ lavas from the 1970s and 1980s that are thought to be derived directly from the SC magma body of the summit reservoir (Pietruszka et al. 2015; 2018). In contrast, the Nb/Y ratios of the phase 1E lavas are similar to summit and ERZ lavas from the 1960s. This was the last time since the late nineteenth century that the summit reservoir is known to have contained magma with an average Nb/Y ratio of ~ 0.68 (Pietruszka and Garcia 1999; Garcia et al. 2003). These observations suggest that the phase 1E magma was derived from the summit reservoir in the 1960s and stored in the ERZ until 2018. Over a period of ~ 50–60 years, this magma differentiated beyond olivine control to ~ 4.8 wt.% MgO (Fig. 7) and low CaO/TiO_2 (Fig. 8c) and Sr/Zr (Fig. 8d) ratios due to fractionation of clinopyroxene and plagioclase (and minor Fe-Ti oxides to raise its K_2O/TiO_2 ratio; Fig. 8b).

The high Nb/Y ratios of the phase 1E lavas must be related to their original parental magma composition from the 1960s, rather than crystal fractionation of clinopyroxene, plagioclase, or Fe-Ti oxides (see the Supplementary Information for a detailed justification). Briefly, clinopyroxene fractionation is the only process that can potentially increase the Nb/Y ratio of the residual melt; neither plagioclase (not shown) nor Fe-Ti oxide (Fig. 8b) fractionation will significantly affect this ratio. The maximum effect of clinopyroxene fractionation on the Nb/Y (~ 0.08) and K_2O/TiO_2 (≤ 0.01) ratios—illustrated for an average parental magma from the 1960s (gray bar trend on Fig. 8b)—is too small to create the phase 1E magma with ~ 4.8 wt.% MgO by differentiation of a parental magma similar to recent Pu'u 'Ō'ō or Halema'uma'u lavas. In fact, the magnitude of such fractionation is likely smaller than the calculated maximum based on a comparison with the differentiated ERZ lavas from 1977 (~ 5.4 wt.% MgO) and sample 1–54 from episode 1 of the Pu'u 'Ō'ō eruption in 1983 (~ 6.1 wt.% MgO). Each of these samples have Pb and Sr isotope ratios that closely match summit and rift lavas from the 1960s (Pietruszka et al. 2018). Thus, they are probably remnants of magma that intruded the ERZ from the summit reservoir at that time (with subsequent storage and differentiation for ~ 14 and 19 years, respectively). The Nb/Y ratios of the differentiated 1977 and 1983 lavas plot well within the range of the 1960s summit and rift lavas (Fig. 8a), indicating that clinopyroxene fractionation had only a minor effect on Nb/Y down to at least ~ 5.4 wt.% MgO.

The composition of the phase 1E lavas—and specifically, the association of their relatively high Nb/Y ratios with 1960s summit and rift lavas—suggests that the first stage of magma mixing prior to the 2018 rift eruption occurred within the ERZ, rather than the summit reservoir. The summit reservoir is an unlikely long-term storage location

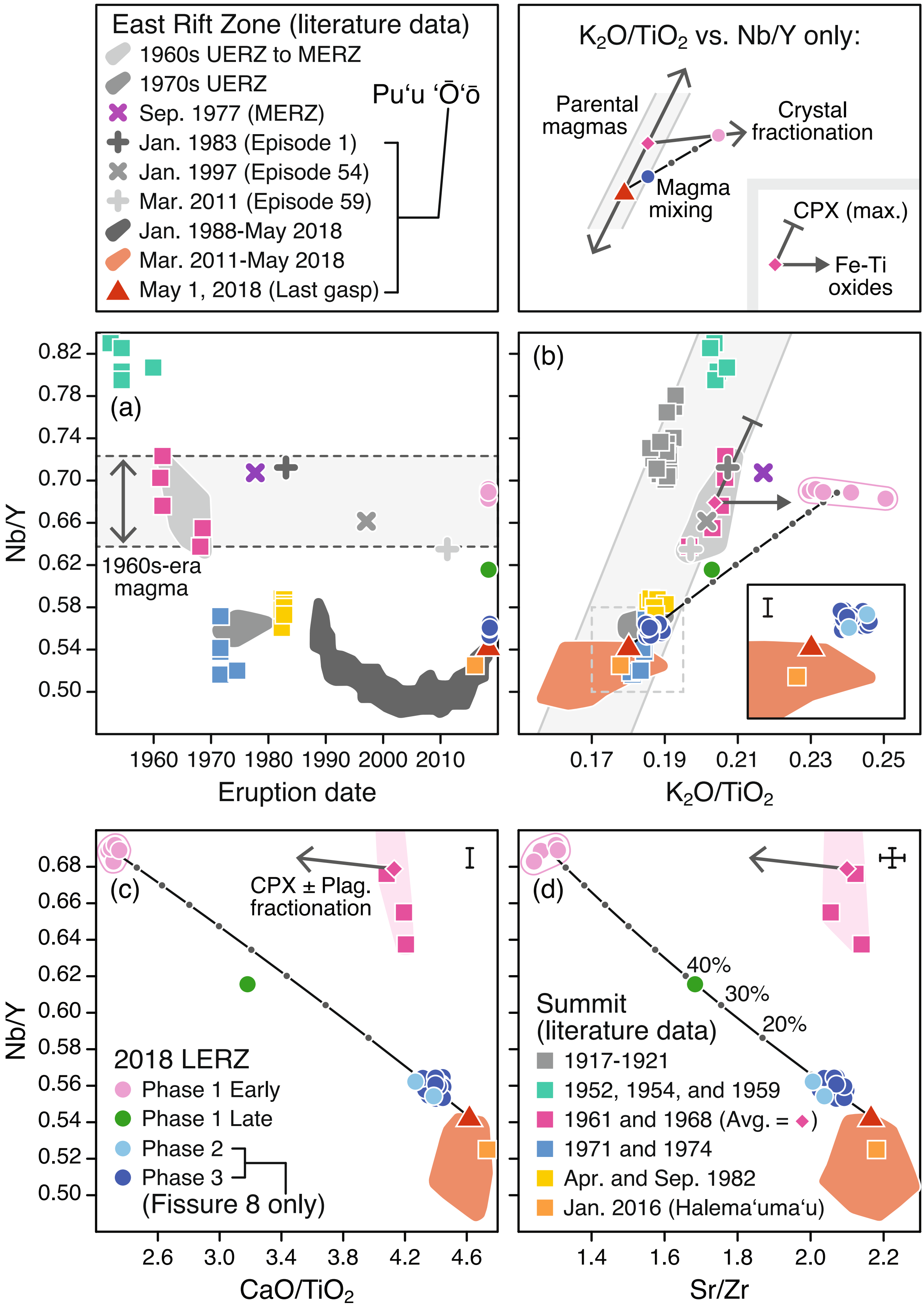
East Rift Zone (literature data)
1960s UERZ to MERZ
1970s UERZ
Sep. 1977 (MERZ)
Jan. 1983 (Episode 1)
Jan. 1997 (Episode 54)
Mar. 2011 (Episode 59)
Jan. 1988-May 2018
Mar. 2011-May 2018
May 1, 2018 (Last gasp)
Pu‘u ‘Ō‘ō
K2O/TiO2 vs. Nb/Y only:
Parental magmas
Crystal fractionation
Magma mixing
CPX (max.)
Fe-Ti oxides
(a)
1960s-era magma
Nb/Y
Eruption date
(b)
K2O/TiO2
(c)
CPX ± Plag. fractionation
2018 LERZ
Phase 1 Early
Phase 1 Late
Phase 2
Phase 3
(Fissure 8 only)
CaO/TiO2
(d)
40%
30%
20%
Summit (literature data)
1917-1921
1952, 1954, and 1959
1961 and 1968 (Avg. = ◆)
1971 and 1974
Apr. and Sep. 1982
Jan. 2016 (Halema‘uma‘u)
Sr/Zr

◀**Fig. 8** Variations in olivine-incompatible major and trace element ratios for Kīlauea lavas. The temporal evolution in Nb/Y for key summit and rift lavas since the mid-twentieth century is shown in (**a**). The Nb/Y ratios of these samples and summit lavas from 1917 to 1921 are plotted against K_2O/TiO_2 in (**b**). Plots of Nb/Y vs. CaO/TiO_2 and Sr/Zr for lavas from the 2018 rift eruption and recent samples from Halemaʻumaʻu (2016 and 2017) and Puʻu ʻŌʻō (2018) are shown in (**c**) and (**d**). Data from Supplementary Table S2 are compared with literature data, as follows. Data sources for Puʻu ʻŌʻō lavas are listed in the caption to Fig. 7. Samples from the main episodes of this eruption (dark gray field) are plotted starting in 1988—when the final amount of 1982-era magma was flushed from the volcano's summit reservoir (Pietruszka et al. 2018)—to emphasize the temporal changes in the composition of the parental magma delivered to Kīlauea. The data for the historical summit and other rift lavas are from Garcia et al. (2003) and Pietruszka et al. (2018), respectively. The historical summit lavas in (**a**) and (**b**) from 1971, 1974, and 1982 include only samples that are inferred to have erupted from the SC magma body (Fig. 2) of the summit reservoir (Pietruszka et al. 2015). Similarly, three rift-stored lavas from the early parts of the two phases of the Mauna Ulu UERZ eruption from 1969 to 1971 and 1972 to 1974 are excluded (Pietruszka et al. 2018). These choices were made to emphasize the changes in parental magma composition at Kīlauea, rather than the temporal delay in the eruption of lava with a given Nb/Y or K_2O/TiO_2 ratio due to its storage time in the HMM magma body of the summit reservoir (Fig. 2) or the UERZ. The maximum possible effect of ~ 22 wt.% clinopyroxene fractionation on the Nb/Y and K_2O/TiO_2 ratio of an average 1960s-era summit magma (gray bar) is shown in (**b**). See the Supplementary Information for details. Fractionation of Fe-Ti oxides would increase the K_2O/TiO_2 ratio of a magma in the direction of the gray arrow in (**b**). A total of ~ 0.8 wt.% ilmenite fractionation would explain the average K_2O/TiO_2 difference between the 1960s summit lavas and phase 1E lavas from the 2018 rift eruption. Magma mixing trends are shown in (**c**) and (**d**) between the May 2018 "last gasp" Puʻu ʻŌʻō lava and the average of the phase 1E lavas from the 2018 rift eruption. The small gray circles show 10 wt.% increments of magma mixing. The inset in (**b**) expands the area within the dashed gray box to highlight the small compositional difference between the MgO-rich 2018 LERZ lavas and recent samples from Puʻu ʻŌʻō and Halemaʻumaʻu. Ratios of major or trace elements are in proportions of wt.% or ppm, respectively. The 2SD error bar for Nb/Y and Sr/Zr is shown; the other error bars are smaller than the size of the symbols

because it was extensively flushed with mantle-derived magma since the 1960s (Pietruszka et al. 2015, 2018) via sustained eruptions on the upper ERZ (UERZ) at Mauna Ulu from 1969 to 1974 and the MERZ at Puʻu ʻŌʻō from 1983 to 2017. The ERZ is the most likely location within Kīlauea's plumbing system that could have stored a significant amount of 1960s-era magma for ~ 50–60 years and allowed for prolonged magma accumulation and mixing prior to the 2018 rift eruption. A series of intrusions from the summit reservoir to the ERZ in the 1960s (Wright and Klein 2014) is thought to have left behind a relatively large amount of magma to serve as a prominent mixing component in subsequent rift lavas based on high-precision Pb and Sr isotope ratios (Pietruszka et al. 2018). The isotopic signature of this 1960s-era magma was observed as a mixing component in the Mauna Ulu eruption and as the dominant component in MERZ eruptions from 1977 and episode 1 of the Puʻu ʻŌʻō eruption in 1983. Samples of differentiated lava from episodes 54 (January 1997) and 59 (March 2011) of the Puʻu ʻŌʻō eruption near Nāpau Crater (Fig. 2), each with an average of ~ 6.2 wt.% MgO, have relatively high Nb/Y (Fig. 8a) and K_2O/TiO_2 (Fig. 8b) ratios that plot within the range of summit lavas from the 1960s (only the low-MgO end member from episode 59 is shown). These Nāpau eruptions are thought to have tapped compositionally heterogeneous pods of decades-old magma (rather than a single, homogeneous body of stored magma) that cooled and differentiated beneath the ERZ at depths of ~ 2–3 km, and for episode 59 in March 2011, mixed with contemporaneous MgO-rich Puʻu ʻŌʻō magma (Walker et al. 2019). In summary, the Pb and Sr isotope ratios (Pietruszka et al. 2018) and/or chemistry (e.g., Nb/Y) of rift lavas from 1977, 1983, 1997, and 2011 suggest that differentiated 1960s-era magma was still available within the MERZ (prior to 2018) to serve as a mixing component for the MgO-rich 2018 LERZ lavas.

Ratios of olivine-incompatible elements in the MgO-rich 2018 LERZ lavas are consistent with this mixing scenario. Summit lavas from the 1960s had high Nb/Y ratios (~ 0.68 on average), and high CaO/TiO_2 (Fig. 8c) and Sr/Zr (Fig. 8d) ratios that are characteristic of olivine-controlled Kīlauea magma. The latter two parameters are lower for the differentiated MERZ lavas from 1977 to 2011 (not shown), and especially, the phase 1E lavas from the 2018 rift eruption. The decrease in CaO/TiO_2 is caused by the fractionation of clinopyroxene ± plagioclase, whereas the decrease in Sr/Zr is caused by plagioclase fractionation (because Sr is compatible and Zr is highly incompatible in plagioclase). The MgO-rich 2018 LERZ lavas have relatively high Nb/Y ratios and low CaO/TiO_2 and Sr/Zr ratios compared to recent samples from Puʻu ʻŌʻō or Halemaʻumaʻu. These chemical signatures can be explained by mixing between a rift-stored, 1960s-era magma that fractionated both clinopyroxene and plagioclase (now represented by the phase 1E lavas) and the "last gasp" Puʻu ʻŌʻō sample (in agreement with the major element abundances shown on Fig. 7). The mixing model (Supplementary Table S3) gives low residuals for the Nb/Y and Sr/Zr ratios of the MgO-rich 2018 LERZ lavas on a sample-by-sample basis.

Location and size of the ERZ magma body

The distinctive chemistry of the MgO-rich 2018 LERZ lavas requires a different location for magma mixing prior to the 2018 rift eruption than the summit reservoir or the ERZ conduit between the summit reservoir and Puʻu ʻŌʻō (Fig. 2). The most likely location was within the MERZ at a depth of ~ 2–4 km, just downrift of Puʻu ʻŌʻō (dashed blue box on Fig. 9a) because (1) the locus of deformation (Neal et al. 2019) and seismicity (Lengliné et al. 2021) for the dike propagation in 2018 initiated near Puʻu ʻŌʻō and then moved ~ 20 km downrift into the LERZ and (2) the CO_2 entrapment depths of olivine-hosted melt inclusions in the MgO-rich 2018 LERZ lavas are nearly all < 5 km (Wieser et al. 2021; Lerner et al. 2021). Alternate locations, such as a deeper portion of the ERZ down to ~ 10 km (Delaney et al. 1990; Lin et al. 2014) and a greater length of such deep magma accumulation from the UERZ to the LERZ, cannot be completely ruled out. However, the relatively low S content of the magma from phase 3 of the 2018 rift eruption suggests that it was degassed via Halemaʻumaʻu lava lake from 2008 to 2018 (Fig. 2) and recycled into the shallow plumbing system (Lerner et al. 2021). Lerner et al. (2021) suggest that much of this degassed magma remained within the summit reservoir or the ERZ uprift of Puʻu ʻŌʻō, but it may have also intruded the ERZ downrift of Puʻu ʻŌʻō.

The compositional homogeneity of the MgO-rich 2018 LERZ lavas suggests that the first stage of mixing occurred in a magma body that was larger than the lava volume erupted from fissure 8 during phase 3. Estimates for the volume of the entire eruption (mostly during phase 3) are ~ 0.8 km^3 (Neal et al. 2019), 0.9–1.4 km^3 (Dietterich et al. 2021), and ~ 2.3 km^3 (Kern et al. 2020). Olivine crystals in the MgO-rich 2018 LERZ lavas with relatively high Fo contents (> 81.5) mostly crystallized, and trapped their CO_2, at depths of ~ 2–4 km (Wieser et al. 2021; Lerner et al. 2021). If this range is assumed to represent the vertical extent of a dike-shaped magma body, the ~ 0.8–2.3 km^3 of lava implies a minimum width of ~ 40–100 m for a ~ 10-km-long dike (Fig. 9a) or ~ 80–200 m for a ~ 5-km-long dike. Efficient magma mixing (Fig. 7) and homogenization (Fig. 3) prior to the 2018 rift eruption would be favored by a shorter, wider dike.

A large amount of magma must have accumulated within the ERZ prior to 2018. The mixing model requires ~ 91–95 wt.% recent summit-derived magma (via Puʻu ʻŌʻō), which corresponds to ~ 0.7–2.1 km^3 of MgO-rich magma based on the estimated range in the volume of lava from the 2018 rift eruption (Neal et al. 2019; Kern et al. 2020; Dietterich et al. 2021). It would take ~ 5–40 years to accumulate this volume if ~ 50% of the magma that intruded the ERZ at a supply rate of ~ 0.1–0.3 km^3/yr (Dvorak and Dzurisin 1993; Poland et al. 2012; Anderson and Poland 2016) during the Puʻu ʻŌʻō eruption remained beneath the surface. For comparison, Dvorak and Dzurisin (1993) estimated that ~ 40% of the magma that intruded the ERZ over the three decades since ~ 1960 never erupted. A time scale of ~ 10 years for the accumulation of this magma would be consistent with (1) the observation from major (Fig. 7) and trace (Fig. 8) elements that Puʻu ʻŌʻō or Halemaʻumaʻu lavas erupted from 2011 to 2018 represent a suitable mixing end member for the MgO-rich 2018 LERZ lavas (although slightly older summit-derived magma cannot be completely ruled out) and (2) the inferred process of shallow magma degassing and recycling via Halemaʻumaʻu lava lake from 2008 to 2018 (Lerner et al. 2021). Independent evidence from ground deformation may support the idea that magma was able to leak downrift of Puʻu ʻŌʻō prior to the 2018 rift eruption (Patrick et al. 2020), including (1) the inflation of the MERZ since ~ 2012 and (2) a gradual large-scale displacement of the south flank of the volcano (~ 8 cm/yr).

Petrogenetic model for the 2018 rift eruption and implications for volcanic behavior

Our new interpretation of the magmatic evolution of Kīlauea's plumbing system prior to (Fig. 2) and during (Fig. 9) the 2018 rift eruption is illustrated using a series of schematic cross sections. From ~ 2008 to 2018, olivine-controlled magma from the summit reservoir supplied two simultaneous eruptions (Poland et al. 2014). Magma from the deeper SC body fed the Puʻu ʻŌʻō eruption, whereas magma from the shallower HMM body (itself connected to the SC body) fed the lava lake within Halemaʻumaʻu (Fig. 9a). The eruption of differentiated lavas with relatively high Nb/Y ratios (Fig. 8a) on the MERZ in 1977 (near the future location of Puʻu ʻŌʻō) and during the Puʻu ʻŌʻō eruption (1983, 1997, and 2011, near Nāpau Crater) indicates that leftover 1960s-era magma was still present within the ERZ prior to 2018 (yellow patches of magma on Fig. 2). This differentiated 1960s-era magma was likely also stored within the ERZ downrift of Puʻu ʻŌʻō (Fig. 9a). The rate of magma delivery from the summit reservoir to the ERZ may have been greater than the rate of eruption prior to 2018 (Anderson and Poland 2016), allowing a large amount of summit-derived magma to accumulate within the MERZ and mix with a small amount of differentiated 1960s-era magma (dashed blue box on Fig. 9a). This ~ 10-year process created a large body of relatively homogeneous hybrid magma (> 0.8 km^3) with a chemical signature that was distinct from recent Kīlauea summit and Puʻu ʻŌʻō lavas. Propagation of this magma body as a dike from the MERZ near Puʻu ʻŌʻō to the LERZ in May 2018 (Fig. 9b) may have caused a small amount of syn-eruptive mixing with 1960s-era magma and, thus, created the intermediate hybrid magma (dashed green box on Fig. 9b) that erupted during phase 1L. The first lava to reach the surface on the LERZ during phase 1E was differentiated magma from the 1960s (Fig. 9b), whereas the basaltic andesite to andesite of the easternmost fissure 17 may have been stored beneath the LERZ since the 1955 eruption (Gansecki et al. 2019). The small amount of phase 1 magma (1E followed by 1L) was rapidly flushed from the ERZ by the large intruding dike. The magma within this dike accumulated variable amounts of compositionally

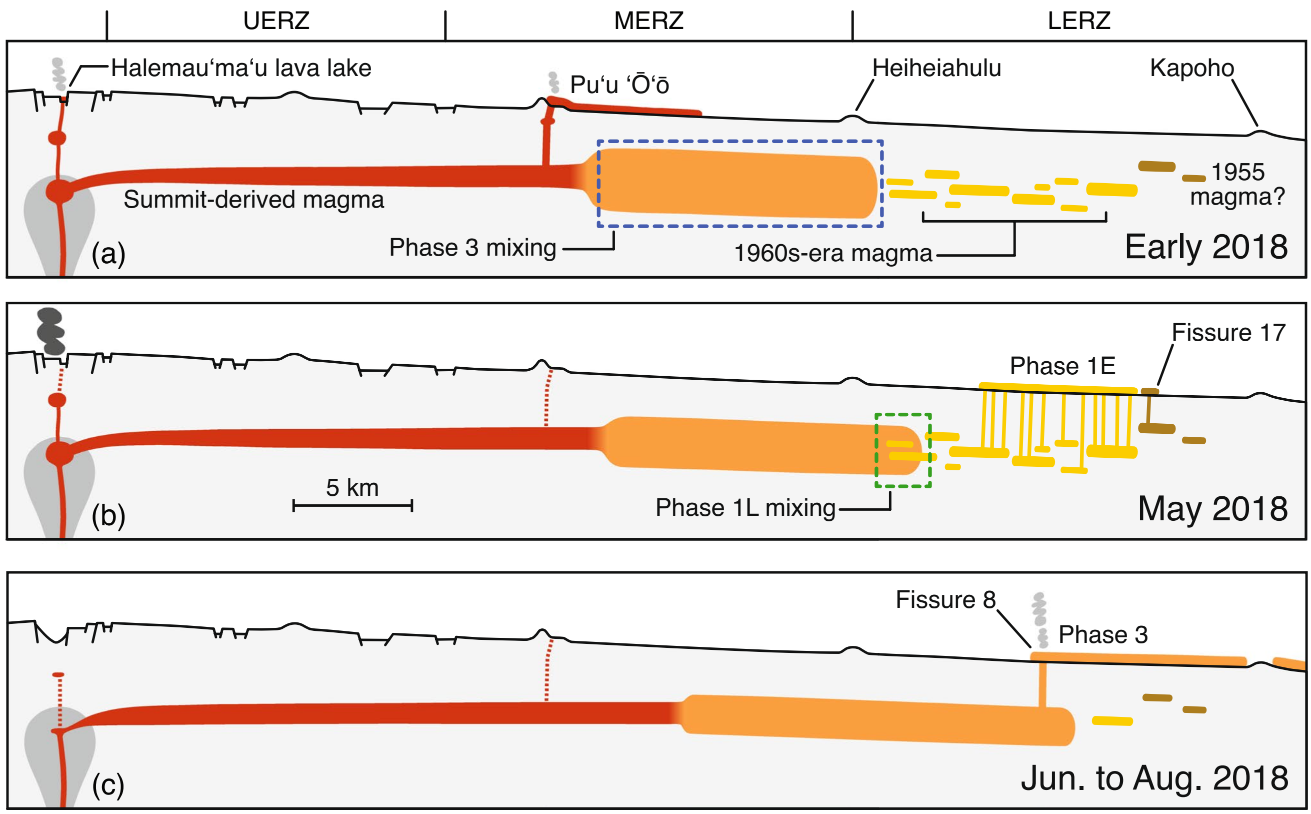

Fig. 9 The magmatic evolution of Kīlauea Volcano illustrated using a series of schematic cross sections: (**a**) early 2018, just prior to the start of the 2018 rift eruption, (**b**) May 2018, during phase 1 of the 2018 rift eruption, and (**c**) June to August 2018, during phase 3 of the 2018 rift eruption. See the text for details

heterogeneous olivine crystals during its rapid and vigorous transport down the ERZ. This two-stage mixture of two magmas plus olivine became the direct source of the MgO-rich 2018 LERZ lavas that erupted from fissure 8 during phases 2 and 3 of the 2018 rift eruption (Fig. 9c). The eruption ceased before any contemporaneous magma from either the summit reservoir or Pu‘u ‘Ō‘ō reached the surface on the LERZ.

This petrogenetic model has implications for the future behavior and potential hazards of Kīlauea Volcano. Our interpretations suggest that a large body of magma (> 0.8 km^3) must have accumulated within Kīlauea's ERZ prior to 2018, most likely within the MERZ downrift of Pu‘u ‘Ō‘ō. This magma body (1) grew cryptically on a time scale of ~ 10 years during the longest rift eruption (~ 35 years) and the only sustained (~ 10 years) dual summit-rift eruption in the recorded history of this volcano and (2) accumulated in a portion of the ERZ that was previously intruded by a substantial amount of summit-derived magma in the 1960s. There is no evidence from the chemistry of the MgO-rich 2018 LERZ lavas that magma from the summit reservoir erupted directly on the LERZ in 2018, despite the strong summit-rift hydraulic connection over ~ 40 km (Patrick et al. 2019a). This implies that (1) most or all of the magma that was removed from the summit reservoir during the caldera collapse in 2018 (up to ~ 0.8 km^3; Anderson et al. 2019), and any leftover Pu‘u ‘Ō‘ō magma, remains within the ERZ and (2) a significant portion of the magma that erupted from fissure 8 on the LERZ in 2018 may yet remain beneath the surface. In addition, the summit reservoir has likely been replenished with magma based on recent lava lake activity within Halema‘uma‘u from December 2020 to May 2021. Thus, Kīlauea's plumbing system from the summit to the LERZ may now be flush with magma and primed for a new era of frequent and/or large eruptions, despite a major caldera collapse and voluminous rift eruption in 2018, and subsequent ~ 2-year eruptive pause. We predict that samples from future ERZ eruptions over a period of years to decades will preserve the chemical signatures (wholly or as mixing end members) of both the MgO-rich 2018 LERZ lavas and the recent (pre-2018) lava that erupted from Pu‘u ‘Ō‘ō and Halema‘uma‘u. A time-series analysis of the changes in lava chemistry at Kīlauea using high-precision Pb and Sr isotope ratios (Pietruszka et al. 2015, 2018)—via the 2018 rift eruption, the 2020–2021 Halema‘uma‘u lava lake, and future eruptions—will be required to determine if the dynamic changes to the volcano's magmatic plumbing system prior to (Fig. 2) or during (Fig. 9) the 2018 rift eruption were ultimately driven by the delivery of a new magma batch from the mantle to a volcanic edifice that already held an unusually large amount of stored magma (Anderson et al. 2019; Patrick et al. 2020). This information will help to determine if Kīlauea is entering a new volcanic cycle of infrequent explosive summit eruptions or continuing its decades-long pattern of nearly continuous effusive activity (Swanson et al. 2014). There is still much to be learned about Kīlauea, one of the world's best understood and most active basaltic volcanoes (Tilling and Dvorak 1993).

Conclusions

The chemical variations of the MgO-rich lavas from Kīlauea's 2018 rift eruption reveal the following insights into the magmatic processes and potential hazards of this frequently active basaltic volcano:

1. The MgO-rich 2018 LERZ lavas are compositionally distinct from recent Puʻu ʻŌʻō lavas, including the "last gasp" sample from May 2018, and lavas from Halemaʻumaʻu in 2016 and 2017. The MgO-rich 2018 LERZ lavas have relatively high K_2O and TiO_2 abundances at a given MgO value, high Nb/Y ratios, and low CaO/TiO_2 and Sr/Zr ratios. These observations preclude a simple hypothesis that the collapse of the caldera in 2018 forced magma from the summit reservoir to erupt directly on the LERZ.
2. The distinctive chemistry of the MgO-rich 2018 LERZ lavas can be explained by mixing between three components that were observed to erupt at Kīlauea: (1) olivine-controlled magma, derived from the summit reservoir via Puʻu ʻŌʻō, (2) differentiated magma similar to the phase 1E lavas from the 2018 rift eruption, and (3) olivine. The differentiated magma was stored within the ERZ since the 1960s. The summit-derived magma (~91–95%) accumulated downrift of Puʻu ʻŌʻō and mixed with the differentiated magma (~5–9%) over ~10 years prior to 2018.
3. The MgO-rich 2018 LERZ lavas are compositionally homogeneous with only ~1 wt.% total range in MgO, and ~2–3% relative variation in MgO-normalized K_2O and TiO_2, CaO/TiO_2, and Nb/Y. The limited variation in the chemical parameters that are insensitive to olivine accumulation or fractionation—despite the large differences in the (inferred) composition of the magma mixing end members—indicates that the MgO-rich 2018 LERZ lavas were well mixed prior to eruption.
4. This mixing process created a large (>0.8 km^3), relatively homogeneous magma body within the MERZ (downrift of Puʻu ʻŌʻō) at a depth of ~2–4 km that was the direct source of the MgO-rich 2018 LERZ lavas.
5. The magma that was removed from the summit reservoir during the caldera collapse in 2018 (up to ~0.8 km^3) remains within the ERZ, along with any leftover magma from the Puʻu ʻŌʻō and 2018 rift eruptions. The summit reservoir has likely been replenished with magma based on recent lava lake activity within Halemaʻumaʻu from December 2020 to May 2021. Thus, Kīlauea's plumbing system from the summit to the LERZ may now be flush with magma and primed for a new era of frequent and/or large eruptions.

In summary, our detailed study of the petrogenetic history of the MgO-rich 2018 LERZ lavas shows that the size, location, and interconnectedness of shallow magma bodies at Kīlauea changed dynamically on a time scale of only ~10 years during simultaneous eruptions at Puʻu ʻŌʻō and Halemaʻumaʻu. A geochemical and isotopic time-series analysis of lavas from recent past and future Kīlauea eruptions will help to decipher the underlying role of deeper magmatic processes—such as the delivery of new batches of mafic magma from the mantle—on the eruptive behavior and hazards of this frequently active volcano.

Supplementary Information The online version contains supplementary material available at https://doi.org/10.1007/s00445-021-01470-3.

Acknowledgements This study would not have been possible without the efforts of numerous HVO scientists and volunteers during the response to the volcanic crisis and rift eruption at Kīlauea in 2018. We thank R. Lee, C. Gansecki, and D. Swanson for providing samples and M. Vollinger and K. Ching for assistance with the XRF analyses. A. Mourey and T. Shea shared their ideas about the 2018 rift eruption and helped us refine the logic of our preferred model. Detailed comments and helpful suggestions by P. Wallace, an anonymous reviewer, and the editors (N. Métrich and A. Harris) are gratefully acknowledged. This is SOEST contribution #11348.

Author contribution M.O.G. designed the study, made the petrographic observations, and prepared the whole-rock powders for analysis. J.M.R. performed the XRF analyses. A.J.P. expanded upon the early interpretations of M.O.G. and J.M.R., modeled the data, drafted the figures, and wrote the manuscript in collaboration with M.O.G. and J.M.R.

Funding This work was supported by grants from the National Science Foundation (20–11366 to A. Pietruszka and A. Greene, and 18–38502 to K. Rubin, M. Garcia, J. Hammer, and T. Shea).

References

Anderson KR, Poland MP, Johnson JH, Miklius A (2015) Episodic deflation-inflation events at Kīlauea Volcano and implications for the shallow magma system. In: Carey RJ, Cayol V, Poland MP, Weis D (eds) Hawaiian Volcanoes: From Source to Surface. AGU, Geophys Monogr 208:229–250

Anderson KR, Poland MP (2016) Bayesian estimation of magma supply, storage, and eruption rates using a multiphysical volcano model: Kīlauea Volcano, 2000–2012. Earth Planet Sci Lett 447:161–171. https://doi.org/10.1016/j.epsl.2016.04.029

Anderson KR, Johanson IA, Patrick MR, Gu M, Segall P, Poland MP, Montgomery-Brown EK, Miklius A (2019) Magma reservoir failure and the onset of caldera collapse at Kīlauea Volcano in 2018. Science 366:eaaz1822. https://doi.org/10.1126/science.aaz1822

Bemelmans MJW, de Zeeuw-van DE, Poland MP, Johanson IA (2021) Insight into the May 2015 summit inflation event at Kīlauea Volcano Hawaiʻi. J Volcanol Geotherm Res 415:107250. https://doi.org/10.1016/j.jvolgeores.2021.107250

Bjarnason IT, Cowie P, Anders MH, Seeber L, Scholz CH (1993) The 1912 Iceland earthquake rupture: growth and development of a nascent transform system. Bull Seis Soc Am 83:416–435

Chen K, Smith JD, Avouac J-P, Liu Z, Song YT, Gualandi A (2019) Triggering of the Mw 7.2 Hawaiʻi earthquake of 4 May 2018 by a dike intrusion. Geophys Res Lett 46:2503–2510. https://doi.org/10.1029/2018GL081428

Clague DA, Moore JG, Dixon JE, Friesen WB (1995) Petrology of submarine lavas from Kīlauea's Puna Ridge, Hawaiʻi. J Petrol 36:299–349

Clague DA, Hagstrum JT, Champion DE, Beeson MH (1999) Kīlauea summit overflows: their ages and distribution in the Puna District, Hawaiʻi. Bull Volcanol 61:363–381

Delaney PT, Fiske RS, Miklius A, Okamura AT, Sako MK (1990) Deep magma body beneath the summit and rift zones of Kīlauea Volcano, Hawaiʻi. Science 247:1311–1316

Dietterich HR, Diefenbach AK, Soule SA, Zoeller MH, Patrick MP, Major JJ, Lundgren PR (2021) Lava effusion rate evolution and erupted volume during the 2018 Kīlauea lower East Rift Zone eruption. Bull Volcanol 83:25. https://doi.org/10.1007/s00445-021-01443-6

Dvorak JJ (1992) Mechanism of explosive eruptions of Kīlauea Volcano, Hawaiʻi. Bull Volcanol 54:638–645

Dvorak JJ, Dzurisin D (1993) Variations in magma supply rate at Kīlauea Volcano, Hawaiʻi. J Geophys Res 98:22255–22268

Fiske RS, Kinoshita WT (1969) Inflation of Kīlauea Volcano prior to its 1967–1968 eruption. Science 165:341–349

Fiske RS, Rose TR, Swanson DA, Champion DE, McGeehin JP (2009) Kulanaokuaiki Tephra (ca. A.D. 400–1000): newly recognized evidence for highly explosive eruptions at Kīlauea Volcano. Hawaiʻi Geol Soc Am Bull 121:712–728. https://doi.org/10.1130/B26327.1

Gansecki C, Lee RL, Shea T, Lundblad SP, Hon K, Parcheta C (2019) The tangled tale of Kīlauea's 2018 eruption as told by geochemical monitoring. Science 366:eaaz0147. https://doi.org/10.1126/science.aaz0147

Garcia MO, Ho RA, Rhodes JM, Wolfe EW (1989) Petrologic constraints on rift-zone processes: results from episode 1 of the Puʻu ʻŌʻō eruption of Kīlauea Volcano, Hawaiʻi. Bull Volcanol 52:81–96

Garcia MO, Rhodes JM, Wolfe EW, Ulrich GE, Ho RA (1992) Petrology of lavas from episodes 2–47 of the Puʻu ʻŌʻō eruption of Kīlauea Volcano, Hawaiʻi: evaluation of magmatic processes. Bull Volcanol 55:1–16

Garcia MO, Rhodes JM, Trusdell FA, Pietruszka AJ (1996) Petrology of lavas from the Puʻu ʻŌʻō eruption of Kīlauea Volcano: III. The Kupaianaha episode (1986–1992). Bull Volcanol 58:359–379

Garcia MO, Pietruszka AJ, Rhodes JM, Swanson K (2000) Magmatic processes during the prolonged Puʻu ʻŌʻō eruption of Kīlauea Volcano, Hawaiʻi. J Petrol 41:967–990

Garcia MO, Pietruszka AJ, Rhodes JM (2003) A petrologic perspective of Kīlauea Volcano's summit magma reservoir. J Petrol 44:2313–2339. https://doi.org/10.1093/petrology/egg079

Garcia MO, Pietruszka AJ, Norman MD, Rhodes JM (2021) Kīlauea's Puʻu ʻŌʻō eruption (1983–2018): a synthesis of magmatic processes during a prolonged basaltic event. Chem Geol 581:120391. https://doi.org/10.1016/j.chemgeo.2021.120391

Ghiorso MS, Sack RO (1995) Chemical mass transfer in magmatic processes IV. A revised and internally consistent thermodynamic model for the interpolation and extrapolation of liquid-solid equilibria in magmatic systems at elevated temperatures and pressures. Contrib Mineral Petrol 119:197–212

Greene AR, Garcia MO, Pietruszka AJ, Weis D, Marske JP, Vollinger MJ, Eiler J (2013) Temporal geochemical variations in lavas from Kīlauea's Puʻu ʻŌʻō eruption (1983–2010): cyclic variations from melting of source heterogeneities. Geochem Geophys Geosyst 14:4849–4873. https://doi.org/10.1002/ggge.20285

Gualda GAR, Ghiorso MS, Lemons RV, Carley TL (2012) Rhyolite-MELTS: a modified calibration of MELTS optimized for silica-rich, fluid-bearing magmatic systems. J Petrol 53:875–890. https://doi.org/10.1093/petrology/egr080

Kern C, Lerner AH, Elias T, Nadeau PA, Holland L, Kelly PJ, Werner CA, Clor LE, Cappos M (2020) Quantifying gas emissions associated with the 2018 rift eruption of Kīlauea Volcano using ground-based DOAS measurements. Bull Volcanol 82:55. https://doi.org/10.1007/s00445-020-01390-8

Klein FW, Koyanagi RY, Nakata JS, Tanigawa WR (1987) The seismicity of Kīlauea's magma system. In: Decker RW, Wright TL, Stauffer PH (eds) Volcanism in Hawaiʻi, US Geol Surv, Prof Pap 1350:1019–1185

Lengliné O, Duputel Z, Okubo PG (2021) Tracking dike propagation leading to the 2018 Kīlauea eruption. Earth Planet Sci Lett 553:116653. https://doi.org/10.1016/j.epsl.2020.116653

Lerner AH, Wallace PJ, Shea T, Mourey AJ, Kelly PJ, Nadeau PA, Elias T, Kern C, Clor LE, Gansecki C, Lee RL, Moore LR, Werner CA (2021) The petrologic and degassing behavior of sulfur and other magmatic volatiles from the 2018 eruption of Kīlauea, Hawaiʻi: melt concentrations, magma storage depths, and magma recycling. Bull Volcanol 83:43. https://doi.org/10.1007/s00445-021-01459-y

Lin G, Amelung F, Lavallée Y, Okubo PG (2014) Seismic evidence for a crustal magma reservoir beneath the upper east rift zone of Kīlauea Volcano, Hawaiʻi. Geology 42:187–190

Liu C, Lay T, Xiong X (2018) Rupture in the 4 May 2018 MW 6.9 earthquake seaward of the Kīlauea East Rift Zone fissure eruption in Hawaiʻi. Geophys Res Lett 45:9508–9515. https://doi.org/10.1029/2018GL079349

Lynn KJ, Garcia MO, Shea T, Costa F, Swanson DA (2017) Timescales of mixing and storage for Keanakākoʻi Tephra magmas (1500–1820 C.E.), Kīlauea Volcano, Hawaiʻi. Contrib Mineral Petrol 172:76. https://doi.org/10.1007/s00410-017-1395-4

Marske JP, Garcia MO, Pietruszka AJ, Rhodes JM, Norman MD (2008) Geochemical variations during Kīlauea's Puʻu ʻŌʻō eruption reveal a fine-scale mixture of mantle heterogeneities within the Hawaiian plume. J Petrol 49:1297–1318. https://doi.org/10.1093/petrology/egn025

Matzen AK, Baker MB, Beckett JR, Stolper EM (2011) Fe-Mg partitioning between olivine and high-magnesian melts and the nature of Hawaiian parental liquids. J Petrol 52:1243–1263. https://doi.org/10.1093/petrology/egq089

Michon L, Di Muro A, Villeneuve N, Saint-Marc C, Fadda P, Manta F (2013) Explosive activity of the summit cone of Piton de la Fournaise volcano (La Réunion island): a historical and geological review. J Volcanol Geotherm Res 264:117–133. https://doi.org/10.1016/j.jvolgeores.2013.06.012

Neal CA, Brantley SR, Antolik L, Babb JL, Burgess M, Calles K, Cappos M, Chang JC, Conway S, Desmither L, Dotray P, Elias T, Fukunaga P, Fuke S, Johanson IA, Kamibayashi K, Kauahikaua J, Lee RL, Pekalib S, Miklius A, Million W, Moniz CJ, Nadeau PA, Okubo P, Parcheta C, Patrick MP, Shiro B, Swanson DA, Tollett W, Trusdell F, Younger EF, Zoeller MH, Montgomery-Brown EK, Anderson KR, Poland MP, Ball JL, Bard J, Coombs M, Dietterich HR, Kern C, Thelen WA, Cervelli PF, Orr T, Houghton BF, Gansecki C, Hazlett R, Lundgren P, Diefenbach AK, Lerner AH, Waite G, Kelly P, Clor L, Werner C, Mulliken K, Fisher G, Damby D (2019) The 2018 rift eruption and summit collapse of Kīlauea Volcano. Science 363:367–374. https://doi.org/10.1126/science.aav7046

Ort MH, Di Muro A, Michon L, Bachèlery P (2016) Explosive eruptions from the interaction of magmatic and hydrothermal systems during flank extension: the Bellecombe Tephra of Piton de La Fournaise (La Réunion Island). Bull Volcanol 78:5. https://doi.org/10.1007/s00445-015-0998-8

Patrick MR, Dietterich HR, Lyons JJ, Diefenbach AK, Parcheta C, Anderson KR, Namiki A, Sumita I, Shiro B, Kauahikaua JP (2019) Cyclic lava effusion during the 2018 eruption of Kīlauea Volcano. Science 366:eaay9070. https://doi.org/10.1126/science.aay9070

Patrick M, Orr T, Anderson K, Swanson D (2019b) Eruptions in sync: improved constraints on Kīlauea Volcano's hydraulic connection. Earth Planet Sci Lett 507:50–61. https://doi.org/10.1016/j.epsl.2018.11.030

Patrick MR, Houghton BF, Anderson KR, Poland MP, Montgomery-Brown E, Johanson I, Thelen W, Elias T (2020) The cascading origin of the 2018 Kīlauea eruption and implications for future forecasting. Nat Commun 11:5646. https://doi.org/10.1038/s41467-020-19190-1

Pietruszka AJ, Garcia MO (1999) A rapid fluctuation in the mantle source and melting history of Kīlauea Volcano inferred from the geochemistry of its historical summit lavas (1790–1982). J Petrol 40:1321–1342

Pietruszka AJ, Norman MD, Garcia MO, Marske JP, Burns DH (2013) Chemical heterogeneity in the Hawaiian mantle plume from the alteration and dehydration of recycled oceanic crust. Earth Planet Sci Lett 361:298–309. https://doi.org/10.1016/j.epsl.2012.10.030

Pietruszka AJ, Heaton DE, Marske JP, Garcia MO (2015) Two magma bodies beneath the summit of Kīlauea Volcano unveiled by isotopically distinct melt deliveries from the mantle. Earth Planet Sci Lett 413:90–100. https://doi.org/10.1016/j.epsl.2014.12.040

Pietruszka AJ, Marske JP, Heaton DE, Garcia MO, Rhodes JM (2018) An isotopic perspective into the magmatic evolution and architecture of the rift zones of Kīlauea Volcano. J Petrol 59:2311–2352. https://doi.org/10.1093/petrology/egy098

Poland MP, Miklius A, Sutton AJ, Thornber CR (2012) A mantle-driven surge in magma supply to Kīlauea Volcano during 2003–2007. Nat Geosci 5:295–300. https://doi.org/10.1038/ngeo1426

Poland MP, Miklius A, Montgomery-Brown EK (2014) Magma supply, storage, and transport at shield-stage Hawaiian volcanoes. In: Poland MP, Takahashi TJ, Landowski, CM (eds) Characteristics of Hawaiian Volcanoes, US Geol Surv, Prof Pap 1801:179–234

Rhodes JM (1988) Geochemistry of the 1984 Mauna Loa eruption: implications for magma storage and supply. J Geophys Res 93:4453–4466

Rhodes JM, Vollinger MJ (2004) Composition of basaltic lavas sampled by phase-2 of the Hawai'i Scientific Drilling Project: geochemical stratigraphy and magma types. Geochem Geophys Geosyst 5:Q03G13. https://doi.org/10.1029/2002GC000434

Roeder PL, Emslie RF (1970) Olivine-liquid equilibrium. Contrib Mineral Petrol 29:275–289

Shamberger PJ, Garcia MO (2007) Geochemical modeling of magma mixing and magma reservoir volumes during early episodes of Kīlauea Volcano's Pu'u 'Ō'ō eruption. Bull Volcanol 69:345–352. https://doi.org/10.1007/s00445-006-0074-5

Sides IR, Edmonds M, Maclennan J, Swanson DA, Houghton BF (2014) Eruption style at Kīlauea Volcano in Hawai'i linked to primary melt composition. Nat Geosci 7:464–469. https://doi.org/10.1038/ngeo2140

Simkin T, Howard KA (1970) Caldera collapse in the Galápagos Islands, 1960. Science 169:429–437

Staudacher T, Ferrazzini V, Peltier A, Kowalski P, Boissier P, Catherine P, Lauret F, Massin F (2009) The April 2007 eruption and the Dolomieu crater collapse, two major events at Piton de la Fournaise (La Réunion Island, Indian Ocean). J Volcanol Geotherm Res 184:126–137. https://doi.org/10.1016/j.jvolgeores.2008.11.005

Swanson DA, Rose TR, Fiske RS, McGeehin JP (2012) Keanakāko'i Tephra produced by 300 years of explosive eruptions following collapse of Kīlauea's caldera in about 1500 CE. J Volcanol Geotherm Res 215–216:8–25. https://doi.org/10.1016/j.jvolgeores.2011.11.009

Swanson DA, Rose TR, Mucek AE, Garcia MO, Fiske RS, Mastin LG (2014) Cycles of explosive and effusive eruptions at Kīlauea Volcano, Hawai'i. Geology 42:631–634. https://doi.org/10.1130/G35701.1

Teplow W, Marsh B, Hulen J, Spielman P, Kaleikini M, Fitch D, Rickard W (2009) Dacite melt at the Puna Geothermal Venture Wellfield, Big Island of Hawai'i. Geotherm Res Council Trans 33:989–994

Thordarson T, Self S (1993) The Laki (Skaftár Fires) and Grímsvötn eruptions in 1783–1785. Bull Volcanol 55:233–263

Tilling RI, Koyanagi RY, Lipman PW, Lockwood JP, Moore JG, Swanson DA (1976) Earthquake and related catastrophic events, Island of Hawai'i, November 29, 1975: a preliminary report. US Geol Surv Circular 740:1–33

Tilling RI, Dvorak JJ (1993) Anatomy of a basaltic volcano. Nature 363:125–133

Trusdell FA, Wolfe EW, Morris J (2005) Digital database of the geologic map of the Island of Hawai'i. US Geol Surv, Data Ser 144

Tuohy RM, Wallace PJ, Loewen MW, Swanson DA, Kent AJR (2016) Magma transport and olivine crystallization depths in Kīlauea's east rift zone inferred from experimentally rehomogenized melt inclusions. Geochim Cosmochim Acta 185:232–250. https://doi.org/10.1016/j.gca.2016.04.020

Vinet N, Higgins MD (2010) Magma solidification processes beneath Kīlauea Volcano, Hawai'i: a quantitative textural and geochemical study of the 1969–1974 Mauna Ulu lavas. J Petrol 51:1297–1332. https://doi.org/10.1093/petrology.egq020

Walker BH, Garcia MO, Orr TR (2019) Petrologic insights into rift zone magmatic interactions from the 2011 eruption of Kīlauea Volcano, Hawai'i. J Petrol 60:2051–2076. https://doi.org/10.1093/petrology/egz064

Wieser PE, Edmonds M, Maclennan J, Jenner FE, Kunz BE (2019) Crystal scavenging from mush piles recorded by melt inclusions. Nat Commun 10:5797. https://doi.org/10.1038/s41467-019-13518-2

Wieser PE, Lamadrid H, Maclennan J, Edmonds M, Matthews S, Iacovino K, Jenner FE, Gansecki C, Trusdell F, Lee RL, Ilyinskaya E (2021) Reconstructing magma storage depths for the 2018 Kīlauean eruption from melt inclusion CO_2 contents: the importance of vapor bubbles. Geochem Geophys Geosyst 22:e2020GC009364. https://doi.org/10.1029/2020GC009364

Wright TL (1971) Chemistry of Kīlauea and Mauna Loa lava in space and time. US Geol Surv, Prof Pap 735:40

Wright TL, Fiske RS (1971) Origin of differentiated and hybrid lavas of Kīlauea Volcano, Hawai'i. J Petrol 12:1–65

Wright TL, Klein FW (2014) Two hundred years of magma transport and storage at Kīlauea Volcano, Hawai'i. US Geol Surv, Prof Pap 1806:240